



## Harnessing cavitation effects for green process intensification

Zhilin Wu, Silvia Tagliapietra, Alessandro Giraud, Katia Martina, Giancarlo Cravotto\*

Dipartimento di Scienza e Tecnologia del Farmaco, University of Turin, Turin 10125, Italy



### ARTICLE INFO

#### Keywords:

Cavitation phenomena  
Green chemistry  
Process intensification  
Hydrodynamic cavitation  
Ultrasound

### ABSTRACT

The impressive chemo-physical effects observed in sonochemistry are a result of cavitation, as ultrasonic and hydrodynamic cavitation does not interact with matter at the atomic and molecular levels. Bubble collapse leads to the quasi-adiabatic heating of the vapour inside bubbles, giving rise to local hot spots in the fluid. Cavitation thus transforms a mechanical energy into high kinetic energy, which is released in very short bursts that are exploited for green process intensification. This paper reviews relevant applications of hydrodynamic and acoustic cavitation with the aim of highlighting the particular advantages that these phenomena offer to the intensification of green chemical processes. Emulsification, biodiesel preparation, wastewater decontamination, organic synthesis, enzymatic catalysis and extractions are discussed among others. As a comparison, hydrodynamic cavitation technique is more advantageous in dealing with process intensification at large-scale, as well as the enhancement of mass transfer and heat transfer, while ultrasonic cavitation technique is more convenient to operate, easier to control in the studies at lab-scale, and exhibits more efficient in producing active free radicals and inducing the cleavage of volatile compounds.

### 1. Introduction

Cavitation phenomena can be generated via the action of ultrasound (ultrasonic cavitation – UC) [1], and when large pressure differentials are generated within a moving liquid (hydrodynamic cavitation – HC) [2]. The formation, growth, and implosive collapse of either gas or vapour-filled bubbles in liquids cause extreme physical phenomena, such as high pressure and temperature, intense shock waves and microjets, resulting in significant chemical and physical effects [3]. The study of UC's chemical effects, namely sonochemistry, began to attract extensive attention when Richards and Loomis observed the first chemical effects of high frequency sound waves in 1927 [4]. While UC-promoted oxidation was first recorded in 1929 [5,6], HC as a phenomenon was identified earlier when Sir John Thornycroft and Sidney Barnaby observed the rapid motion of propeller blades through water in 1895 [7], while the study of the chemical consequences of HC created during the turbulent flow of liquids began in the 1990s [2,3,8]. Both UC and HC technologies are currently applied in a wide range of green process intensification protocols, including organic synthesis [9,10], nanomaterial fabrication [11], wastewater treatment [12], and biomass valorisation [13], among others. Cavitation processes can provide significant advantages over traditional mixing process. These benefits include enhancing physical and chemical processes, accelerating reactions, and promoting the conversion of raw materials per unit time and

product yield. They thereby achieve the purpose of green chemistry; saving energy and raw materials, reducing by-products and improving production efficiency.

The differences between UC and HC are mainly reflected in different processing scales and input power densities, resulting in differences in reaction rate and energy efficiency. The ultrasound-assisted degradation of organic pollutants in aqueous solution has typically been carried out in a reaction volume of 0.01–0.9 L, and the electrical power density of the horn-batch process has been calculated as 0.53–60 kW L<sup>-1</sup>, while that is 0.13–0.23 kW L<sup>-1</sup> for an ultrasonic bath and 0.43 kW L<sup>-1</sup> for a bench-scale continuous flow reactor [14–16]. Meanwhile, treatment with HC has been performed in 0.8–50 L of volume in a bench-scale batch reactor with an electrical power density of 0.1–0.63 kW L<sup>-1</sup> [17]. It has even been possible to achieve an electrical power density of only ca. 0.007 kW L<sup>-1</sup> over 1 h in a 800 L h<sup>-1</sup> continuous flow reactor combined with ozonation on a pilot scale [18].

This paper reviews applications of HC processes in emulsification, biodiesel preparation and wastewater decontamination, and applications of UC in organic synthesis (heterocycle synthesis, esterification, miscellanea), enzymatic catalysis and extractions in order to highlight the particular advantages that HC and UC offer the field of green chemical process intensification.

\* Corresponding author.

E-mail address: [giancarlo.cravotto@unito.it](mailto:giancarlo.cravotto@unito.it) (G. Cravotto).

<https://doi.org/10.1016/j.ultsonch.2018.12.032>

Received 20 September 2018; Received in revised form 11 December 2018; Accepted 21 December 2018

Available online 22 December 2018

1350-4177/ © 2018 Elsevier B.V. All rights reserved.

## 2. Overview of hydrodynamic cavitation for process intensification

HC is observed when large pressure differentials are generated within a moving liquid [3,19–21]. HC is well-known for its destructive capabilities, including material damage and the generation of intense noise in hydrodynamic engineering, meaning that a large number of previous hydrodynamic studies have attempted to avoid or reduce this cavitation-induced damage [22]. However, HC began to be harnessed as a process intensification technique in the 1990s and saw use in the hydrolysis of fatty oils [2], the polymerisation/depolymerisation of aqueous polymeric solutions [23,24], water disinfection [25] and the preparation of nano-materials [8], among others. HC was then seen as an energy efficient and up-scalable alternative technology for intensification proposes and as being analogous to UC [19].

The fundamental parameter in the description of cavitation is the cavitation index:

$$\sigma = \frac{P_0 - P_v}{\frac{1}{2}\rho U_0^2} \quad (1)$$

where  $P_0$  and  $U_0$  are the characteristic pressure and velocity respectively,  $\rho$  is the density, and  $P_v$  is the vapour pressure of liquid [26].

The equation for the cavitation index indicates that hydrodynamic cavitation is produced by the pressure variation in a flowing liquid that is caused by a variation of velocity in the system [27]. Since the pressure differential within a moving liquid is the critical factor, the cavitation number  $\sigma$  can simply be defined by following equation:

$$\sigma = \frac{P_d - P_v}{P_u - P_d} \approx \frac{P_d}{P_u} \quad (2)$$

where  $P_d$ ,  $P_u$  and  $P_v$  are the downstream, upstream, and vapour pressures, respectively. The approximation holds when  $P_d \geq P_u \geq P_v$ . An increase in upstream pressure or a decrease in downstream pressure should decrease  $\sigma$  and increase the number of cavitation events [3,28].

Cavitation is generally not possible unless  $\sigma$  is less than 1.0 and is expected to be more intense at lower  $\sigma$  values [29]. HC can simply be generated by the passage of the liquid through a restrictor [21,30]. A typical HC reaction system generally consists of a centrifugal pump, a restrictor, a heat exchanger, a reservoir, flow meters, manometers, valves and connecting pipes, as shown in Fig. 1. A range of restrictors,

including throttling valves, orifice plates and venturi, etc. have been used to produce HC. Some commonly used restrictors are listed in Table 1, while liquid whistles, rotor-stator homogenizers and high-pressure jet fluidizers also see frequent use [3,31–33].

Hole diameter ( $r$ ), upstream pressure ( $P_u$ ) and downstream pressure ( $P_d$ ) are the most important effective factors when using a restrictor to produce HC, while geometrical parameters, such as the  $\alpha$ ,  $\beta$  and  $\beta_0$  values, are also critical: parameter  $\alpha$  is defined as the ratio of the total hole perimeter to the total flow area; dimensionless geometrical parameter  $\beta$  is defined as the ratio of hole diameter to pipe diameter; dimensionless parameter  $\beta_0$  is defined as the ratio of total flow area to the cross sectional area of the pipe [42].

The fields of mechanical material processing, chemical and pharmaceutical processing, food and biological processing and wastewater treatment have all extensively developed and explored HC technology in recent decades. Physical processing mainly includes the emulsification, dispersion and homogenization of heterogeneous phases [35], the crystallization and preparation of nano-materials [43,44], flotation [45] and leaching [46]. Chemical processing includes organic synthesis [47–49], polymerisation and depolymerisation [50,51], the upgradation of crude oil and vacuum residue [52], deep desulphurisation of liquid fuels [53]. Food and biological processing includes milk production [54,55], the extraction of nutrient and bioactive compounds [56,57], cell disruption, disinfection and the inactivation of microalgae [17,25,58], extraction for bio-resources, as well as delignification, bioethanol and biogas preparation [59–61]. Water and wastewater treatment includes water disinfection [17,25,62], microalgae inactivation [58], and wastewater decontamination [34,63–65].

## 3. Emulsification and homogenization via hydrodynamic cavitation

Emulsification, defined as the process of dispersing one liquid into a second immiscible liquid, is a common process in food, nutraceutical, cosmetic, pharmaceutical and chemical processing. The type of simple emulsion that is produced (water-in-oil or oil-in-water, commonly abbreviated as w/o and o/w) is mainly dictated by the volume ratio of the two liquids, their order of addition and the nature of the emulsifier [66]. Besides mechanical stirring (MS) and UC [67], HC can be used to provide energy via a number of methods, namely rotor-stator type mixers [33–68], high-pressure homogenizers [69], throttling valve mixers [35], orifice plate and venturi mixers [36], cavitation mixers [70], liquid whistles [31], and two-stage orifice valves [40]. An oil-in-water emulsion created using HC is shown in Fig. 2.

The collapse of a cavitation bubble near the liquid-liquid boundary causes the drops in the disperse phase to break up and thus favours the emulsification process [70]. The effects that other parameters, such as the density difference between the dispersed and continuous phases, the viscosity of the two liquids, surfactant type, homogenizer design, electrostatic and/or steric repulsion between droplets, and the volume, size and volume ratio of the two phases, have on the performance of emulsification have been discussed in detail in previous studies [33,67,70]. Importantly, Emulsions are characterized by emulsion droplet size, while emulsion stability also depends on droplet size [33]. The effect that HC has on the average droplet size and its distribution are thus explored herein.

Rotor-stator homogenisers, characterized by their highly localized energy dissipation, are widely used in process industries for dispersed-phase size reduction and reactive mixing [68]. In this case, emulsion droplet size is mainly determined by the shear forces and HC generated in the turbulent zone. The size of these droplets generally decreases with increasing homogenization intensity and duration. A final equilibrium emulsion droplet size of around 1  $\mu\text{m}$  has been obtained in 10 mL of a 0.4  $\text{g mL}^{-1}$  Poly(methyl methacrylate)/methylene chloride solution with 2 mL of 0.2  $\text{g mL}^{-1}$  aqueous bovine serum albumin solution after 1 min of processing in which the homogenization intensity

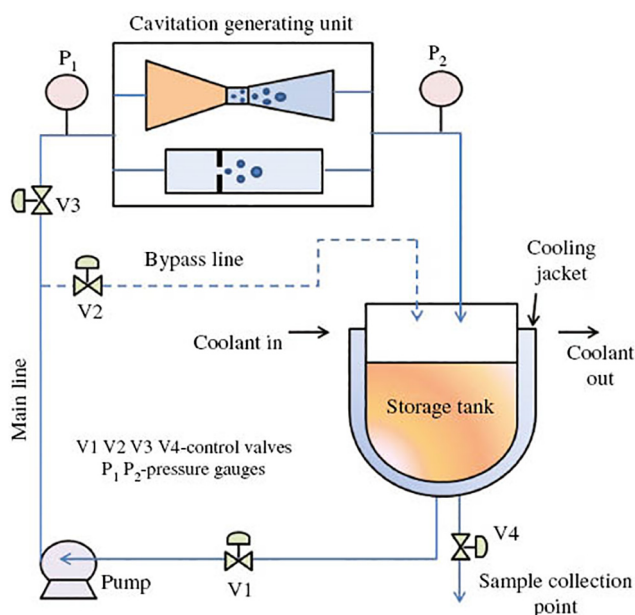





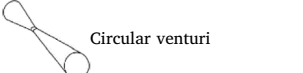
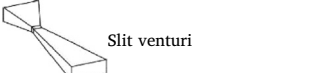
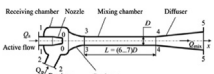
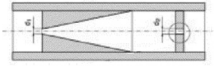
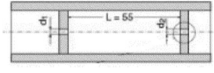
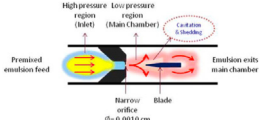
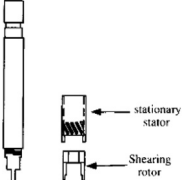
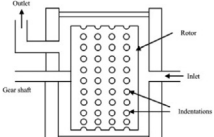
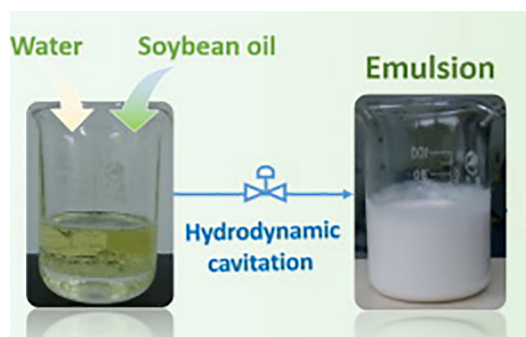


Fig. 1. Schematic of a HC reaction system. Reprinted from ref. [34]. Copyright (2016), with permission from Degruyter.

**Table 1**  
Forms of various restrictors used to produce HC.

Restrictor	Common form	Variant form	Ref.
Throttling valve			[35]
Orifice plate (OP)	Single hole 	Multi-orifice 	[36,37]
Venturi	Circular venturi 	Slit venturi 	[36]
Venturi-Cylindrical array	Venturi array 	Cylinder Array 	[38]
Cavitation mixer			[39]
Two-stage orifice valve			[40]
Liquid whistle			[41]
Rotor–stator homogenizer			[32,33]



**Fig. 2.** Oil-in-water emulsification using HC. Reprinted from ref. [35], Copyright (2016), with permission from Elsevier.

exceeded 10,000 rpm [33].

A high-pressure homogenizer (operating at 20,000 psi) shows a much higher energy dissipation value, of  $2 \times 10^7 \text{ W kg}^{-1}$ , than a high-speed rotor-stator homogenizer (energy dissipation  $4.2 \times 10^3 \text{ W kg}^{-1}$ ) [70]. Cavitation effects are very important for droplet disruption during emulsification in high-pressure homogenizers. Droplets can be deformed by shear flow forces and subsequently disrupted by turbulent or cavitating flow. 1 vol% vegetable oil-in-water emulsions have been produced using Tween 80 in a high-pressure homogenizer, at 10 MPa, equipped with a two-stage orifice valve. The minimum droplet diameter

that was achieved under optimal values was about  $0.7 \mu\text{m}$ . Use of the maximum HC intensity not only led to the most efficient droplet disruption and smallest droplet size, but also to a narrow droplet size distribution with a large fine fraction [40].

Traditional methods, such as rotor–stator type mixers and high-pressure homogenizers, have reached the limits of their potential. For example, the lowest particle sizes produced in rotor–stator type mixers are in the 1–2  $\mu\text{m}$  range, while the use of high-pressure homogenizers (up to 275 MPa) causes problems for the safety and reliability of the equipment, maintenance, energy consumption and scale up that are difficult to overcome [70]. Controlled Flow Cavitation™ technology was developed by Five Star Technologies (Cleveland, OH), and reported in 1999. The very high levels of energy dissipation produced during the collapse of a large number of cavitation bubbles allow the mixer to generate very small particle sizes and very uniform particle size distributions. Emulsions are produced at relatively low operating pressures, making the scale up of the cavitation mixer easier and less costly to achieve. The deagglomeration of suspensions and emulsions of various drop sizes, from the submicron scale to 5  $\mu\text{m}$ , are accomplished at operating pressures from 1 to over 7 MPa [70]. The droplet sizes and polydispersity indices (PDI) of oil-in-water emulsions that have been obtained using various HC devices are listed in Table 2.

A mustard oil-(10%) in-water nanoemulsion with a droplet size of 87 nm was created in the presence of 8% surfactants (Span 80 and Tween 80) using low pressure hydrodynamic cavitation (LPHC) at 1 MPa. Moreover, the kinetic stability of the nanoemulsion was assessed

**Table 2**  
Droplet size and PDI of oil-in-water emulsions obtained using various HC devices.

HC type	Orifice size (mm)	Upstream pressure (MPa)	Emulsifier	Average droplet size ( $\mu\text{m}$ )	PDI	Ref.
Ultra-Turrax (T18 Basic) and high-pressure liquid whistle Sonolator™	1.6	1.4	Span 80	< 0.6	< 0.4	[31]
Throttling valve		0.8		0.027	0.006	[35]
Low pressure HC device	1–3	1.0	Tween 80, Span 80	0.087	0.1	[36]
Controlled Flow Cavitation™	nozzle	< 1.0		1.0–5.0		[70]
		1.0–6.9		0.5–2.0		
		> 6.9		< 1.0		
High-Pressure Homogenizers with two-stage orifice valve	0.5 and 0.8	< 15	Tween 80	< 0.8	0.7	[40]
High-pressure liquid whistle	1.0	5.5	Tween 80, Span 80	< 0.5	0.5	[41]

Note: PDI, Polydispersity index, is a dimensionless measure of size distribution width that is calculated from a cumulant analysis and ranges from 0 to 1.0. A small PDI value (< 0.08) indicates a near monodisperse population, while a large PDI (> 0.7) indicates a very broad droplet size distribution.

under centrifugal and thermal stress conditions and was found to be unaffected. Furthermore, the nanoemulsion is physically stable for up to 3 months. Importantly, HC was proven to be 11 times more energy efficient than UC for the preparation of the nanoemulsion [36]. The slit venturi method was the best restrictor for the reduction of droplet size, and was followed by the circular venturi and orifice plate methods that had the same  $\beta$  value. The smallest droplet size was obtained at the optimum  $P_u$  (1 MPa) and  $\sigma$  (0.19) values after 90 min of processing time. The orifice plate, which has a large  $\beta$  value, provides a larger shear layer area and, as a result, generates more cavities and smaller droplet sizes, while the  $\alpha$  value does not significantly affect the droplet size [36]. However, the only droplet size achieved was 215 nm in the coconut oil-in-water emulsion prepared using the venturi at 1 MPa of  $P_u$  and 16–0.23 of  $\sigma$  [71].

Furthermore, refined soybean oil-, heptane- and castor oil-in-deionised water emulsions (O/W 0.2 L/2 L) have been prepared in the presence of 1.25% sodium dodecyl sulfate using LPHC, giving average O/W emulsion droplet sizes of 27, 68 and 19 nm, respectively, at 0.83 MPa. Droplet size decreases with increases in inlet pressure, number of cavitation passes and surfactant concentration. The emulsion exhibited admirable physical stability, which lasted 8 months [35].

Palm oil-based submicron emulsions have been prepared for the encapsulation of curcumin in the presence of Tween 80 using a liquid whistle hydrodynamic cavitation reactor (LWHCR). A minimum droplet size of 476 nm and a PDI of 0.5 were achieved using an orifice plate-blade distance of 0.6 cm and an inlet operating pressure of 5.5 MPa. Moreover, a curcumin encapsulation efficiency of 88% was achieved using the optimum operating conditions for submicron emulsion generation. The final droplet size for curcumin-loaded submicron emulsions was 532 nm [41]. This LWHCR system also produced highly stable W/O/W multiple emulsions containing ferrous fumarate on a submicron scale (< 600 nm) and a droplet-size distribution PDI in the narrow regime. The physical stability of the W/O/W emulsions increased significantly with operating pressure and number of emulsification passes [31].

#### 4. Biodiesel preparation via hydrodynamic cavitation

While several renewable energy sources have been developed over the last 40 years, biodiesel is able to play a particularly important role as its high heating values are nearly equivalent to those of diesel fuels and it has a low environmental impact. The sustainability of the biodiesel preparation process is closely related to the type of oil source used and to overall energy consumption [72]. Biodiesel has unique properties, including biodegradability, renewability and non-toxicity. It has reduced sulphur oxide and greenhouse gas emissions as it produces lower amounts of carbon- and sulphur- based gases than conventional fossil fuels [73].

Non-edible oils, such as nagchampa, karanja, jatropa, neem and cotton, and waste sources, such as waste vegetable oil and waste-

cooking oil (WCO), are considered to be good feedstocks for biodiesel synthesis [30,74], which involves the catalytic conversion of oils to glycerol and acid alkyl ester using methanol. However, this process has an inherent drawback; mass transfer resistance results in a lower reaction rate, with high energy, time and production costs [30,72,73]. Intensification technologies, such as microwave, UC and HC reactors, have been widely used to eliminate the mass transfer resistance caused by the immiscible reactants. Recent studies have revealed that microwave and ultrasonic cavitation techniques are not yet completely feasible for biodiesel production on an industrial scale, but also that HC offers a number of advantages over other intensification technologies. In general, yield efficiency increased in the following order, in relation to the method used: HC > MW > UC > mechanical stirring (MS) [73].

As mentioned above, the physical effects of HC, including microemulsification and streaming, eliminate the mass transfer resistance in the process, since cavitation effects increase the interfacial area of contact between methanol and the triglyceride molecules [30,75]. HC has been proven to be energy efficient as an intensification technology, is capable of converting oil to methyl ester in lower reaction times and can reduce overall production costs. Moreover, HC-prepared biodiesel can be used as fuel in diesel engines [74]. For example, 98% WCO conversion was achieved using HC under optimum conditions; a 1:6 WCO-to-methanol molar ratio in the presence of 1 wt% KOH at 60 °C for 15 min. Triglyceride conversion follows pseudo-first order kinetics. Reaction rate constants were 0.238 and 0.031 min<sup>-1</sup>, while activation energies were 89.7 and 92.7 kJ mol<sup>-1</sup> using HC and MS, respectively. Yield efficiency and energy efficiency were 8.33 and 1.8 times, respectively, higher than those of MS, and reaction time and feedstock input are 6 times shorter and 4.6 times lower when using HC [74]. The pretreatment of high-free-fatty-acid rubber seed oil via esterification using a pilot-scale HC reactor (50 L) has demonstrated that HC was 4 times more efficient than MS and that processing time was 3 times shorter than that of MS, giving the same conversion [76]. This evidence proves that the HC process is a time saving, energy efficient and environmentally-friendly technology, compared to the conventional MS process [30,74]. As far as biodiesel quality is concerned, HC-produced thumba oil-based biodiesel can be used as an alternative fuel giving better performance and lower emissions than diesel. A 30% biodiesel blend of thumba oil shows higher brake power, brake thermal efficiency, as well as reduced smoke and pollutant emissions compared to diesel. Moreover, the HC biodiesel production process is a simple, efficient, time saving, eco-friendly and industrially viable process [77]. Pre-blended equi-volume oils mixtures have been prepared by HC method. Biodiesel properties, such as kinematic viscosity, density, pour point, flash point and acid value, fulfil ASTM D6751 and EN 14214 standards. The kinematic viscosity, acid value and flash point of HC-produced biodiesel are lower than those of biodiesels produced using the MS and UC methods, which can be attributed to the higher purity of the final product [30,78,79].



Higher free fatty acid (FFA) contents can be found in WCO and non-edible oil feedstocks, such as nagchampa and rubber seed oil. If a higher-FFA feedstock directly undergoes a base transesterification reaction, saponification will occur, meaning that the FFA content in these feedstocks must be reduced to less than 1% via the acid esterification process before transesterification. The HC process can also be used to reduce FFA content as a pretreatment [79].

#### 4.1. Comparison of UC and HC

Both the UC and HC methods have been proven to be efficient and to save time and energy in the preparation of biodiesel via the transesterification of plant oil. The HC process can generate similar cavitating conditions to UC and even has a better effect on mixing immiscible liquids [10,80]. Moreover, intensification degree depends on the uniform distribution of cavitation activity. UC activity is non-uniform and decreases with distance from the transducer surface, whereas the physical effects of HC are uniformly distributed throughout the reactor [21,81]. Furthermore, the scale-up of HC to industrial-scale operation appears to be more beneficial than that of the UC process as HC is easier to generate and is less sensitive to the geometry of the reactor. The energy consumption values of transesterification via MS, UC and HC, relative to the production of 1 kg biodiesel from soybean oil, are 0.50, 0.25 and 0.18 kWh, respectively. HC is clearly the most efficient, both in terms of time and energy [10,80]. Another significant advantage that HC has over UC and MS is that it can operate under ambient temperature and pressure conditions. A reaction temperature that is close to the boiling point of methanol is required for reaction initiation under MS alone, whereas similarly high temperatures are also required to avoid the attenuation effects of high liquid viscosity under UC [30,82].

The esterification of fatty acids (FA) odour cut ( $C_8$ – $C_{10}$ ) with methanol in the presence of concentrated  $H_2SO_4$  has been performed by HC and UC. Ambient temperature and pressure operating conditions and reaction times of < 3 h are sufficient to give > 90% conversions (mol%) for all the different combinations of acid (lower and higher)/methanol. This clearly establishes the efficacy of cavitation as an excellent way to achieve the process intensification of biodiesel synthesis [83]. However, for the esterification of Karanja oil, with an initial acid value of 14.15 mg of KOH  $g^{-1}$  of oil, the maximum reduction in acid value (2.7 mg of KOH  $g^{-1}$  of oil) was obtained using UC at an optimum oil-to-methanol molar ratio of 1:5 and with 2% sulphuric acid loading at ambient temperature. The acid value was reduced to 4.2 mg of KOH  $g^{-1}$  of oil under optimized HC conditions in first stage processing [84].

A biodiesel yield of more than > 96.5% was obtained from the transesterification of rapeseed oil with methanol in a combined HC and UC process in a single-step reaction with only one second of hydraulic residence time in the cavitation reactor. The optimal conditions included  $\beta$  0–8.4%, an oil to methanol ratio of 4:1, 125  $\mu$ m ultrasonic amplitude, 0.5 wt% catalyst and 45 °C [85]. Cavitation yields, i.e. biodiesel yield per unit energy consumption, provided by HC, UC and MS have often been compared to identify which process gives the best energy efficiency. A comparison of HC, UC and MS cavitation yields

can be seen in Table 3.

As shown in Table 3, the cavitation yield of HC is several times higher than those of UC or MS. On the one hand, with same input mass of oil it requires much less reaction time to reach the maximum yield by using HC process as compared with using MS [79,87]. On the other hand, more biodiesel can be produced by using HC reactor than using ultrasound reactor for the same reaction time [78,83]. The conditions, conversions and cavitation yields for the synthesis of biodiesel from various feedstocks using various HC devices are summarized in Table 4.

#### 4.2. Effect of HC type and effective factors

As shown in Table 4, the effects of HC device configuration, geometry and reaction conditions on the conversion and kinetics of transesterification have been recently studied. HC devices include rotor-stator, high speed homogenizer, venturi and OP-type HC devices for the synthesis of biodiesel. Reaction conversions and biodiesel yields show significant differences over the same reaction period because of differences in the power dissipated into the system [78]. The flow geometry of orifice plates plays a crucial role in process intensification. Upstream pressure significantly affects the rate of formation of methyl esters from used frying oil. Using an optimized plate geometry of 2 mm hole diameter and 25 holes, more than 95% triglycerides was converted into methyl esters in 10 min at a cavitation yield of  $1.28 \times 10^{-3} g J^{-1}$  [37].

#### 4.3. Effect of various HC configurations

High speed homogenizer (HSH): the high-speed rotation of the reactor creates micron-sized droplets of the immiscible reacting mixture and leads to outstanding mass and heat transfer, enhancing the kinetics of the transesterification reaction which completes much more quickly than with traditional methods [90]. HSH (T25 Ultra Turrax, IKA) with a rotor-stator has recently been used at a rotation speed range of 3000–25,000 rpm for the intensification of biodiesel synthesis from soybean oil and WCO. After pretreatment (esterification), the acid value of WCO was reduced from 27 mg of KOH  $g^{-1}$  of oil to 1.5 mg of KOH  $g^{-1}$  of oil. The transesterification of soybean oil and esterified WCO was performed in the presence of a heterogeneous catalyst (CaO) using HSH. The maximum biodiesel yield, 84% for soybean oil with 3 wt% CaO, and 88% for WCO with 1 wt% CaO, was obtained under the optimal conditions, which were a molar ratio of oil to methanol of 1:10 at 50 °C and 12,000 rpm of rotation speed in 30 min. Significant increases in the rate of biodiesel production were observed upon using HSH, as compared to the conventional MS method, which requires 2–3 h for a similar biodiesel yield. The intensification provided by HSH is attributed to the turbulence caused at the microscale and the generation of fine emulsions, which is favoured by the cavitation effects [92].

In another study, the maximum biodiesel yield obtained was 97% for WCO and 92.3% using HSH (MA102, 18.5 kW) from fresh sunflower oil under optimized conditions; reaction time of 120 min, methanol-to-oil molar ratio of 12:1, 3% wt KOH catalyst at 50 °C. The equipment can be operated at a flow range of 0.3–0.9  $m^3 h^{-1}$  and at a rotation speed of

**Table 3**  
A comparison of HC, UC and MS cavitation yields.

Oil	Mass of Oil (L)			t* (min)			Oil/MeOH (mol/mol)	Catalyst	T (°C)	Cavitation yield (g $kJ^{-1}$ )			Ref.
	HC	UC	MS	HC	UC	MS				HC	UC	MS	
WCO with methyl acetate	4	0.05	0.05	30	30	30	1/12	1% $CH_3OK$	40	1.22	0.048	0.032	[78 86]
FA**	10 mol	0.1 mol	–	–	90	90	1/10	1 wt% $H_2SO_4$	28 ± 2	0.166	0.0245	–	[83]
Palm/Rubber seed oil***	30	–	30	130	–	330	1/8	2 wt% KOH	55	1.35	–	0.008	[79]
WCO	5	–	5	15	–	90	1/6	1 wt% KOH	60	1.25	–	0.15	[87]

t\*: reaction time achieving the maximum yield; \*\*FA: fatty acid, odour cut ( $C_8$ – $C_{10}$ ). \*\*\*Palm/Rubber seed oil: pre-blended equi-volume mixture of crude palm and rubber seed oil.

**Table 4**  
 Synthesis of biodiesel from edible and non-edible oils, and WCO using various HC devices (Note: O/M: molar ratio of oil to methanol; X is conversion of oil).

	HC configuration	Power (KW)	V(L)	P <sub>a</sub> (bar)	t (min)	T (°C)	Oil (g)	O/M (mol/mol)	Catalyst	Cavitational yield (mg J <sup>-1</sup> )	X (%)	Ref.
Soybean oil	OP			7	30	45	100	1/6	1 wt% KOH		~100	[10]
Sunflower oil	OP (24 × 2 mm)		10		40	40	100	1/5	1 wt% NaOH		75	[88]
Rubber seed oil	OP (21 × 1 mm)		50	3	20	50		1/14 (methyl acetate)	0.75 wt% methanolic potassium methoxide	0.83	88	[89]
Rubber seed oil	OP (21 × 1 mm)		50	3	20	55		1/6	1 wt% KOH	0.91	97	[42]
WCO	OP (21 × 1 mm)		50	2	15	60		1/6	1 wt% KOH	1.25	97	[42]
WCO	OP (21 × 1 mm)	4.0	50	2	15	60	5000	1/6	1 wt% KOH	1.25	98	[87]
WCO	OP (21 × 1 mm)	4.0	50	2	15	60	40,000	1/6	1 wt% KOH		98	[74]
Frying oil	OP (25 × 2 mm)	7.5	10	3	10	60		1/6	1 wt% KOH	1.28	95	[37]
Fatty acid odour cut (c8-c10)	OP	1.5	10	ambient conditions	90	28		1/10	1 wt% H <sub>2</sub> SO <sub>4</sub>	1.53–3.1	92	[83]
High acid value non-edible oil from nagchampa	OP	1.5	10	0.69–2.76	60	ambient conditions		1/3	2 wt% H <sub>2</sub> SO <sub>4</sub> for esterification;	acid value:1.6 mg KOH/g oil		[30]
					20	ambient conditions		1/6	1 wt% KOH for transesterification		92	[30]
Pre-blended equi-volume mixture of crude palm and rubber seed oil	OP (1 mm)		50		50	65		1/15	10 wt% H <sub>2</sub> SO <sub>4</sub> for esterification;	FFA content from 25.24% to 0.2%		[79]
					20	55		1/8	2 wt% KOH for transesterification	1.35	90	[79]
WCO	slit venturi 3.7 × 0.92 mm rotor-stator	1.5	15	3	30	< 57		1/12 (methyl acetate)	1 wt% potassium methoxide	1.22	90	[78]
Refined and bleached palm oil	rotor-stator	7.5	7.5		15 + 15	55		1/0.23 (v/v)	3.67 g/L NaOH	8.15	99	[90]
WCO	rotor-stator		7.5		15 + 15	55		1/0.25 (v/v)	5.67 g/L NaOH	8.15	99	[90]
Sunflower oil	high speed homogenizer, 1200–3500 rpm	18.5			120	50		1/12	3 wt% KOH		92	[91]
WCO	high speed homogenizer, 1200–3500 rpm	18.5			120	50		1/12	3 wt% KOH		97	[91]
Soybean oil	high speed homogenizer, 12000 rpm		0.15		30	50		1/10	3 wt% CaO		84	[92]
WCO	high speed homogenizer, 12000 rpm		0.15		30	50		1/10	1 wt% CaO		88	[92]



Fig. 3. Rotor-stator generator of HC (E-PIC S.r.L.) from the authors' laboratory.

between 1200 and 3500 rpm. HSH offers the advantages of enhanced reaction progress at reduced reaction times and improved separation. HSH can thus be a viable approach for intensified biodiesel production and possibly give favourable economics [91].

The base-catalyzed transesterification (methanol/NaOH) of refined and bleached palm oil and waste vegetable cooking oil has been carried out at 55 °C for 30 min in a commercially available rotor-stator type HC reactor designed by E-PIC S.r.l. (Mongrando, Italy) [93] and equipped with a 7.5 kW electric engine and rotating cylinder (Fig. 3). All the biodiesel samples obtained respect the ASTM standard and present fatty acid methyl ester contents of > 99% m/m from both feedstocks. The electrical energy consumption of the HC reactor is 0.030 kW h per L of produced crude biodiesel, making this innovative technology really quite competitive. The reactor can be easily scaled-up, from producing a few hundred to thousands of litres of biodiesel per hour, and also avoids the risk of orifices clogging with oil impurities, which may occur in conventional HC reactors. Furthermore it requires minimal installation space due to its compact design, which enhances overall security [90].

Venturi and OP: biodiesel yields of 64% for the orifice plate, 82% for the circular and 89% for the slit venturi have been obtained while other conditions were kept constant. These results are attributed to the

variations in the power dissipated into the system, which is almost 1.1 times higher for the slit venturi than for circular venturi and 1.5 times higher than for orifice plate. In addition, the slit venturi provides a higher volumetric flow rate for a given pressure drop and lower  $\sigma$  than the orifice plate and circular venturi. The number of cavitation events and their intensity increase with a decrease in  $\sigma$  and these cavitation events are responsible for the formation of local turbulence, liquid micro-circulation and micro-emulsion, which ultimately enhance the biodiesel yield [78].

#### 4.4. Effect of upstream pressure.

The rate of transesterification generally increases with an increase in lower  $P_u$  in venturi and OP-type HC, but beyond a certain pressure there is no significant increase in the rate of reaction and conversion. This can either be because there is no significant improvement in cavitation effect beyond the optimal  $P_u$ , or because the state of choked cavitation has occurred. Moreover, the complete elimination of mass transfer resistance occurs at the optimal  $P_u$  and chemical reactivity becomes the overall rate controlling step. An increase in upstream pressure results in increases in the velocity through the orifice. As the amount of liquid passing through the orifice per unit time increases, the number of passes of liquid through the cavitating zone also increases, leading to better conversion. Increases in the upstream pressure also lead to an increase in the pressure drop across the orifice plate, thereby increasing cavity collapse intensity, and improving the mass transfer between immiscible phases [37].

For example, as  $P_u$  increases from 2 to 3 bar with a slit venturi, the biodiesel yield from WCO increases from 79% to 89% with a 1:1.2 M ratio of oil to methyl acetate. However, further increases in inlet pressure, from 3 to 4 bar, provide no significant increases in biodiesel yield [78]. The effect of upstream pressure on the conversion of a variety of oils is listed in Table 5. As can be seen, 3 bar appears to be the optimal  $P_u$  for most biodiesel production using HC processes.

#### 4.5. Effect of parameter $\alpha$

The value of  $\alpha$  depends on the number and size of the holes. With same flow area, plates with the highest number of holes and the smallest hole size (larger value of  $\alpha$ ) give better conversion, since a higher number of holes increases the cavity and shear layer area. The higher  $\alpha$  value results in an improved cavitation effect and lower resistance to mass transfer, and therefore, better emulsification [37]. The maximum conversion of used frying oil was obtained at the highest  $\alpha$  value. With the same  $\beta_0$  value, the conversion at an  $\alpha$  value of 0.4 is about 77%, while an  $\alpha$  value of 1.33 gives 97% conversion at  $P_u$  1.5 bar and 60 °C for 20 min. For the conversion of WCO, the maximum conversion was 97% with a 21 × 1 mm orifice plate ( $\alpha = 4.00 \text{ mm}^{-1}$ ), at  $P_u$  2 bar and 60 °C for 15 min [37]. The effect of  $\alpha$  value on the conversion of a variety of oils is detailed in Table 6.

Table 5

The effect of upstream pressure on the conversion of various oils.

Oil type and major reaction conditions	Hole	Pu (bar)								Ref.
		No OP	1.0	1.5	2.0	3.0	3.5	4.0	5.0	
Used frying oil, 60 °C, 20 min, 1:6 of molar ratio of oil to methanol, 1% KOH	OP, 1 × 10 mm	40	74	77	87	93	–	–	–	[37]
WCO, 60 °C, 15 min, 1:6 of molar ratio of oil to methanol, 1% KOH	OP, 21 × 1 mm	35	83	–	97	97	–	–	–	[42]
WCO, 60 °C, 20 min, 1:12 of molar ratio of oil to methyl acetate, 1% potassium methoxide	Slit venturi, 3.7 × 0.92 mm	–	–	–	68	78	–	80	70	[78]
Rubber seed oil, 55 °C, 20 min, 1:6 of molar ratio of oil to methanol, 1% KOH	OP, 21 × 1 mm	–	88	–	90	97	97	–	–	[94]
Rubber seed oil, 50 °C, 40 min, 1/14 (methyl acetate), 0.75 wt% methanolic potassium methoxide	OP, 21 × 1 mm	–	68	–	82	88	89	–	–	[76]

**Table 6**  
The effect of  $\alpha$  value on the conversion of various oils.

Oil type and major reaction conditions	Hole	$\beta_0$	$\alpha$ (mm <sup>-1</sup> )	Conversion (%)	Ref.
Used frying oil, 1.5 bar, 60 °C, 20 min	1 × 10 mm	0.25	0.4	77	[37]
	25 × 2 mm	0.25	2.0	97	
	16 × 3 mm	0.36	1.33	83	
	20 × 3 mm	0.45	1.33	94	
WCO, 2.0 bar, 60 °C, 15 min	1 × 4.58 mm	0.09	0.87	54	[42]
	21 × 1 mm	0.09	4.00	97	
	9 × 2 mm	0.16	2.00	89	
	5 × 3 mm	0.20	1.33	67	
Rubber seed oil, 3.0 bar, 55 °C, 20 min	1 × 4.58 mm	0.09	0.87	64	[76]
	21 × 1 mm	0.09	4.00	97	
	9 × 2 mm	0.16	2.00	85	
	5 × 3 mm	0.20	1.33	83	

#### 4.6. Effect of parameter $\beta_0$ value

An optimal  $\beta_0$  value generally exists for reaction conversion. The frequency and intensity of turbulence can be improved using plates with a larger number of holes of smaller size. However, very low  $\beta_0$  values result in a lower number of passes of liquid through the cavitating zone and a shorter time in the cavitating zone, leading to worse conversions. The effect of  $\beta_0$  value on the conversion of various oils is detailed in Table 6. As can be seen, the highest conversions of used frying oil (97%), WCO (97%) and rubber seed oil (97%), were obtained at optimal  $\beta_0$  values of 0.25, 0.09 and 0.09, respectively. It is worth noting that conversion increases with  $\beta_0$  value at the same  $\alpha$  value. At the same  $\beta_0$  value, having multi-orifices is favourable to conversion [37].

#### 4.7. Wastewater treatment via hydrodynamic cavitation

Advanced Oxidation Processes (AOPs), such as ozonation, Fenton oxidation, photocatalysis and cavitation processes have all been considered effective technologies for the treatment of bio-refractory contaminants in wastewater in recent decades. In AOPs, non-biodegradable organic molecules are broken up into smaller molecules, which can be further degraded by conventional biological technologies [95–98]. The principal mechanism of AOPs is the generation of highly reactive free radicals. As a close relative of UC, HC can drive local hotspots with extreme collapse temperatures and pressures in very short times, not only inducing the direct cleavage of volatile organic molecules in or around the hotspots, but also cracking water molecules to produce OH radicals [3,99–102].

As compare with UC, HC provides substantially lower individual cavity collapse intensity as assessed in an investigation of the chemical effect of cavitation on triiodide formation (Weissler reaction). The HC induced by a venturi at 8.7 bar had a maximum efficiency of about  $5 \times 10^{-11} \text{ mol J}^{-1}$  for the formation of triiodide, while the maximum was almost  $8 \times 10^{-11} \text{ mol J}^{-1}$  for UC at 24 kHz. Thus UC provides significantly higher Weissler reaction rates [3,29].

The removal efficiency (RE) of 1 mM chloroform in 1.5 L aqueous solution using UC alone (850 kHz, 120 W) and HC alone (1.1 kW) has been directly compared in one HC/US combined system [103]. The RE of chloroform by using UC (70%) is much higher than that using HC (about 7%) for 30 min treatment at the optimum conditions. Also, UC presented remarkably higher energy efficiencies (EE) than HC ( $4.5 \mu\text{mol kJ}^{-1}$  vs  $0.4 \mu\text{mol kJ}^{-1}$ ). Similarly, EEs using UC alone and HC alone were also compared for the degradation of 0.2 mM halogen compounds ( $\alpha$ -chlorotoluene,  $\alpha$ -bromotoluene, chlorobenzene, bromobenzene, chloroform and carbon tetrachloride) at the same scale (800 mL of aqueous solutions) at 20 °C. As a result, the EEs by 850 kHz UC alone is much higher than those by HC treatment under the optimal conditions [102]. Although it is debatable whether HC process has

higher efficiency than UC process for the degradation of organic contaminants [104,105], it can certainly be affirmed that the volume treated using HC process is much higher and the input power density is lower than that using UC reactor, thus HC is more suitable for treating much larger effluent as compared to UC reactor [106]. More importantly, HC process affords a superior opportunity to raise the removal rate and efficiency of contaminants by the combination with other oxidants such as  $\text{H}_2\text{O}_2$ ,  $\text{Na}_2\text{S}_2\text{O}_8$ , NaClO [64,107–110].

As shown in Table 3, the cavitation yield of HC is several times higher than those of UC or MS. The synergy between HC and UC has been seen to occur in the combination process; the bubbles generated by HC become nuclei for UC. The initiation of new cavitation events becomes increasingly difficult as gases are removed from the solution by the implosions of cavitation bubbles (degassing effect). Bubbling gases through the solution facilitates the production of cavitation bubbles via the provision of excess nuclei [111,112]. HC can also enhance ozone mass transfer synergistically under acidic conditions, while the enhancement achieved by the chemical effects of cavitation was about double the enhancement achieved by mechanical effects. The  $k_{La}$  value (diffusion coefficient of ozone) of a single ozonation process with a radical scavenger was  $1.02 \times 10^{-4} \text{ s}^{-1}$ , which became  $1.63 \times 10^{-4} \text{ s}^{-1}$  using venturi HC. Furthermore, without a radical scavenger, the  $k_{La}$  value of the single ozonation process was  $1.53 \times 10^{-4} \text{ s}^{-1}$ , while that figure was  $5.16 \times 10^{-4} \text{ s}^{-1}$  with venturi HC [113]. The existence of dissolved gases lowers the cavitation threshold, which is the minimum energy required for cavitation to be generated. Moreover, microbubbles possess low rising velocity that gives longer ozone residence times [114]. Although, the HC/UC and HC/ $\text{O}_3$  hybrid methods have been successfully used to degrade organic contaminants and inactivate microorganisms in the authors' previous studies [18,103,115–117], the oxidative degradation of organic contaminants using HC alone, HC/ $\text{H}_2\text{O}_2$  and HC/Fenton methods are highlighted in this review.

#### 4.8. Degradation of organic contaminants by HC alone

HC can destroy microorganisms and cause cell disruption, which both drive the disinfection of water and wastewater, by inactivating bacteria and zooplankton, including microalgae [17,25,58,118–120]. HC can also drive the thermal cleavage of volatile organics, such as chloroform, tetrachloromethane, benzene, toluene, ethylbenzene and xylene in aqueous solution at room temperature [101,121]. Importantly, it can also produce active radicals. The formation of OH radicals has been proven to occur at high upstream pressure (150–1500 bar) and lower upstream pressure (6.9–275 bar). No oxidation of 1.0 M KI was observed in aqueous solution when using high-pressure jet fluidizers, below 150 bar of hydrostatic pressure. Over 150 bar, the triiodide formation rate increased with increased hydrodynamic pressure [3]. For the same reaction, no OH radicals were produced when using an orifice plate device and salicylic acid as the dosimeter at an upstream pressure of < 100 psi (6.9 bar), but excellent results were obtained with a small circular nozzle at 4000 psi (275 bar) [100]. This indicates that HC device type and configuration dominate the formation rates of OH radicals. In other study, even below 6.9 bar of hydrodynamic pressure, organic pollutants, such as alachlor, can be efficiently oxidized under 0.2–0.6 MPa (2–6 bar) in aqueous solution in a swirling jet cavitation reactor. Also, the degradation rates of alachlor increased with increasing pressure [122].

Degradation using HC generally follows pseudo-first-order kinetics. Operating parameters, such as HC device type and configuration, upstream pressure, solution temperature, initial concentration and pH value, can affect the formation rates of the OH radical and degradation rates [123]. \*\*\*

It is necessary to note that some studies have suggested that HC is more energy efficient and that it gives higher degradation than UC at equivalent power/energy dissipation levels [123]. Our studies have



**Table 7**  
Comparison of the organic pollutant degradation efficiency of a variety of HC devices under optimal conditions.

HC device	Pump	Pollutant	C <sub>0</sub> (mg/L)	V (L)	P <sub>u</sub> (MPa)	T (°C)	pH	t (min)	RE (%)	RE <sub>TOC</sub> (%)	Ref.
Swirling jet cavitation reactor	2.5 kW, 3000 rpm	Alachlor	50	25	0.6	40	5.9	100	99	–	[113]
Venturi with 2 mm throat	1.1 kW,	Rhodamine B	10	4	0.48	30	4.78	120	25	–	[124]
			10	4	0.48	30	2.5	120	59	30	
OP with 2 mm hole	1.1 kW,	Rhodamine B	10	4	0.48	30	4.78	120	23	–	[124]
Venturi with 2 mm throat	0.37 kW, 2900 rpm	<i>p</i> -nitrophenol	5000	7	0.29			90	53	–	[125]
OP with 2 mm hole		<i>p</i> -nitrophenol	5000	7	0.29			90	51	–	[125]
OP with 2 mm hole	1.1 kW,	Methyl Parathion	20	4	4	35	3	120	44.4	–	[126]
Venturi		Pharmaceuticals	0.001	1	6			60	14–81	–	[127]
Venturi with 2 mm throat	1.1 kW,	Acid Red 88 Dye	40 (100 uM)	4	5	35	2	120	92	36	[123]

Note: C<sub>0</sub> is the initial pollutant concentration; V is the treatment volume; P<sub>u</sub> is the inlet pressure; t is the reaction time; RE is the pollutant removal efficiency; RE<sub>TOC</sub> is the TOC removal efficiency.

demonstrated that HC, used alone, shows lower removal efficiency in organics degradation and that it should be combined with other AOPs, such as H<sub>2</sub>O<sub>2</sub>, Fenton, photocatalysis, ozonation, UC, etc., thus the oxidative efficiency is to be enhanced [102,103,115,116].

Table 7 shows the organic pollutant degradation efficiency of various HC devices under optimal conditions.

It is necessary to note that some studies have suggested that HC is more energy efficient and that it gives higher degradation than UC at equivalent power/energy dissipation levels [123]. Our studies have demonstrated that HC, used alone, shows lower removal efficiency in organics degradation and that it should be combined with other AOPs, such as H<sub>2</sub>O<sub>2</sub>, Fenton, photocatalysis, ozonation, UC, etc., thus the oxidative efficiency is to be enhanced [102,103,115,116].

#### 4.9. Effect of HC device configuration and upstream pressure

As shown as in Fig. 4, ca. 25% removal efficiency has been obtained for the degradation of Rhodamine B using venturi, while OP gave a value of 22.5% after 2 h running at 4.84 bar. This result was attributed to the lower  $\sigma$  value provided by venturi. At lower  $\sigma$  values, the velocities in the reactor, and hence the number of passes through the cavitating zone, are higher, leading to sufficient residence times within the cavitation zone [124].

Similarly, the maximum degradation of an initial *p*-nitrophenol concentration of 5 g L<sup>-1</sup> was 53.4% using venturi, as compared to 51% using the orifice plate at same operating pressure of 42.6 psi (2.9 bar) [125].

Meanwhile, the degradation rates of Rhodamine B increase with the increase in the inlet pressure, up to an optimum value of 4.8 bar. [124]. Similarly, a critical operating pressure for the degradation of *p*-nitrophenol and the mineralization during the degradation of phenol does exist [125,128]. The optimum inlet pressure for the degradation of acid red 88 dye (AR88) and methyl parathion is 5 and 4 bar, respectively [123,126]. This is attributed to enhanced cavitation activity at higher

pressures, leading to a higher temperature and pressure pulse, as well the enhanced dissociation of the water molecules and a higher concentration of hydroxyl radicals formed *in situ* [129].

#### 4.10. Effect of temperature

For the Weisler reaction, HC is more effective at 10 °C, than at 20 °C and 30 °C, and also at higher upstream pressures [29], while for the degradation of alachlor, the optimal temperature, in the 30–60 °C range, is 40 °C [122]. Increasing temperature from 30 to 40 °C results in a corresponding increase in the degradation of Rhodamine B. It appears that increasing operating temperatures helps to increase the number of cavitation bubbles marginally. However, the effect cannot be generalized, as an increase in temperature also leads to an increase in the vapour pressure of the medium, and to lower cavitation collapse intensity [124]. The degradation of methyl parathion marginally increases as the operating temperature of the system increases from 32 °C to 39 °C [126]. As a result, the increasing temperatures generally favour reaction kinetics but lower the intensity of cavitation collapse. It seems that HC processes can efficiently produce OH radicals at 10–40 °C.

#### 4.11. Effect of initial concentration

The degradation rate of alachlor decreased as the initial concentration increased from 10 to 150 mg L<sup>-1</sup> [122]. The maximum removal for an initial *p*-nitrophenol concentration of 5 g L<sup>-1</sup> was 53.4%, whereas, for 10 g L<sup>-1</sup>, the initial concentration was 44.8% at an operating inlet pressure of 42.6 psi. However, the net mass of *p*-nitrophenol removed is higher at the 10 g L<sup>-1</sup> initial loading than at 5 g L<sup>-1</sup> [125]. Degradation decreases with an increase in the initial concentration of methyl parathion (20–50 mg L<sup>-1</sup>). This is attributed to the insufficient yield of OH radicals produced for a high concentration of substrates, and the competition between substrate and intermediates for reaction with OH radicals [126].

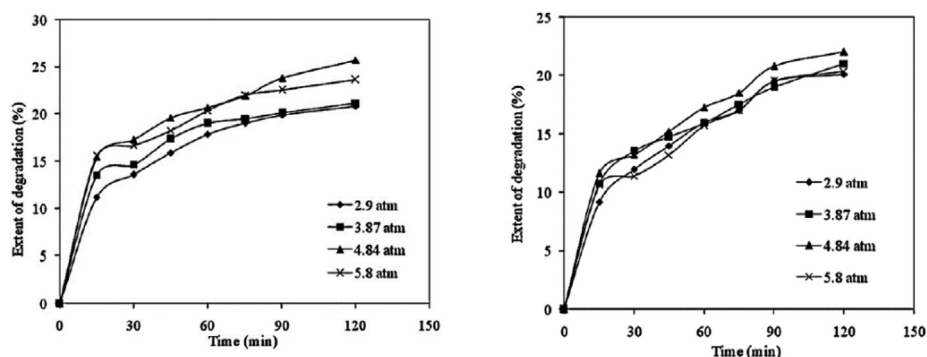


Fig. 4. Degradation of Rhodamine B using venturi (left) and orifice (right) at different inlet pressures. Reprinted from ref. [124] Copyright (2010), with permission from Elsevier.

#### 4.12. Effect of pH value

An increase in rate constants of around 30% has been observed as pH is increased from pH 2 to 12. This is attributed to hydroxide ions in solution inducing increased hydroxyl free radical generation at a high pH value [122]. However, the degradation of Rhodamine B was considerably lower under alkaline and neutral conditions than under acidic conditions. This is attributed to the fact that the generation of hydroxyl radicals via the decomposition of hydrogen peroxide is favoured under acidic conditions; the recombination reaction between free radicals is hampered, thereby increasing the availability of the free radicals. The oxidation capacity of hydroxyl radicals is also higher under acidic conditions.

Furthermore, the degradation of methyl parathion was at its highest at pH 3 in an investigation that ranged from 2.2 to 8.2 [126]. The rate of AR88 decolourisation increases with a decrease in solution pH. A much lower decolourisation rate was observed at pH 10.0, while ca. 92% decolourisation and a 35% reduction in TOC were obtained at pH 2.0 using HC. The dye molecule is present in the molecular state when the pH is less than the  $pK_a$  value (10.7) of AR88, and can then easily enter the gas–water interface of cavities due to its hydrophobic nature, and is thus more readily subjected to OH radical attack and thermal decomposition. In basic medium, however, dye molecules become ionized and hydrophilic in nature and so remain in the bulk liquid. Only about 10% of the OH radicals generated in the cavity can diffuse into the bulk solution [123,130].

#### 4.13. Enhanced effect of HC on oxidation by $H_2O_2$

$H_2O_2$  has been added to a HC system in order to generate more OH radicals. The organic pollutant degradation efficiencies using HC/ $H_2O_2$  are listed in Table 8.

Rhodamine B degradation was enhanced from 59.3%, using venturi alone, to 99.9% in the presence of  $200\text{ mg L}^{-1} H_2O_2$ , while TOC reduction was 55%. Degradation increases with higher  $H_2O_2$  loadings, indicating that more free radical generation occurs at higher  $H_2O_2$  concentrations [124]. The degradation of Rhodamine B also increases with increased  $H_2O_2$  concentration over the 0–150  $\text{mg L}^{-1}$  range in a swirling jet reactor [132].

The degradation of methyl parathion was enhanced from 44.4%, in an operation using only HC, to complete degradation in an operation using a combination of HC and  $200\text{ mg L}^{-1} H_2O_2$ . TOC removal under these conditions was 56.4%. This is attributed to the enhanced formation of the free radicals caused by the continuous dissociation of  $H_2O_2$  under cavitating conditions [126]. Another possibility is that excess  $H_2O_2$  amounts can act as radical scavengers for hydroxyl radicals generated during treatment. The removal of  $1\text{ }\mu\text{g L}^{-1}$  of pharmaceuticals in 1 L aqueous solutions with HC alone and 20 mL of 30%  $H_2O_2$  alone are less effective than those with HC/ $H_2O_2$ , confirming that OH radicals produced during cavitation are primarily responsible for degradation. The amount of  $H_2O_2$  added is clearly important, since the highest removal efficiency was obtained with 20 mL, 30%  $H_2O_2$  per 1 L sample, whereas higher concentrations showed a negative effect on removal [127].

The optimum concentration of  $H_2O_2$  can be considered to be  $4000\text{ }\mu\text{M}$ , which gives a molar ratio of 40:1 ( $H_2O_2$ /AR88). Around 72% TOC reduction and almost 100% colour reduction were obtained in the case of HC with the addition of  $4000\text{ }\mu\text{M } H_2O_2$ , while only 4.6% decolourisation takes place under normal stirring (no HC) with  $H_2O_2$ . The additional  $H_2O_2$  provides the extra hydroxyl radicals for the oxidation of the dye, but also acts as a scavenger of the free radicals generated and therefore the combined effect of HC and  $H_2O_2$  will very much be dependent on the use of the generated free radicals by the dye molecules [123]. Optimal HC/ $H_2O_2$  use resulted in removal efficiencies for Clofibrac acid, Ibuprofen, Naproxen, Ketoprofen, Carbamazepine and Diclofenac of 23%, 19%, 100%, 29%, 89%, 100%, respectively, after

**Table 8**  
Comparison of organic pollutant degradation efficiency of HC/ $H_2O_2$  and HC/Fenton under optimal conditions.

Added oxidant	HC device	Pump	Pollutant	$C_0$ (mg/L)	V(L)	Pu (MPa)	T (°C)	pH	t (min)	RE (%)	RE <sub>roc</sub> (%)	Ref.
$200\text{ mg L}^{-1} H_2O_2$	Venturi with 2 mm throat	1.1 kW	Rhodamine B	10	4	0.48	40	4.78	15	99	55	[124]
$200\text{ mg L}^{-1} H_2O_2$	OP with 2 mm hole	1.1 kW	Methyl Parathion	20	4	4	35	3	120	100	56	[126]
$FeSO_4:H_2O_2$ 1:4	OP with 2 mm hole	1.1 kW	Methyl Parathion	20	4	4	35	3	120	93.8		[126]
$5000\text{ mg L}^{-1} H_2O_2$	Venturi with 2 mm throat	0.37 kW, 2900 rpm	p-nitrophenol	5000	7	0.29			90	60		[125]
$6660\text{ mg L}^{-1} H_2O_2$	Venturi		Pharmaceuticals	0.001	1	6			60	19–100		[127]
$136\text{ mg L}^{-1}$ (4000 $\mu\text{M}$ ) $H_2O_2$	Venturi with 2 mm throat	1.1 kW	Acid Red 88 dye	40 (100 $\mu\text{M}$ )	4	5	35	2	120	99	71	[123]
$FeSO_4:H_2O_2$ 1:5	Venturi with 2 mm throat	0.37 kW, 2900 rpm	p-nitrophenol	5000	7	0.29			90	63		[125]
$FeSO_4:H_2O_2$ 1:5	Venturi with 2 mm throat	1.1 kW	Rhodamine B	10	4	0.48	40	2.5	15	99.9	57	[124]
$Fe^0$ -Fenton, $1900\text{ mg L}^{-1} H_2O_2$	liquid whistle reactor	3.6 kW, 1750 rpm	TOC with phenols	560	4	10.3	$35 \pm 3^\circ\text{C}$	2.5	150		51	[131]
			COD with dye	1680							65	
			TOC with dye	120	4	10.3	$35 \pm 3^\circ\text{C}$	10.4	150		70	
			COD with dye	340					150		85	

Note:  $C_0$  is the initial pollutant concentration; V is the treatment volume;  $P_u$  is the inlet pressure; T is the reaction temperature; t is the reaction time; RE is the pollutant removal efficiency; RE<sub>roc</sub> is the TOC removal efficiency.

60 min running. Coupling the attached-growth biomass biological treatment with the HC/H<sub>2</sub>O<sub>2</sub> process and UV treatment resulted in removal efficiencies of > 90% for clofibrac acid and > 98% for carbamazepine and diclofenac, while the remaining compounds were reduced to levels below the LOD [127].

However, some studies show that the addition of H<sub>2</sub>O<sub>2</sub> gives no significant effect. Six different concentrations of H<sub>2</sub>O<sub>2</sub> (0.05%–1%) have been investigated in a venturi system. The removal of 5 g L<sup>-1</sup> *p*-nitrophenol was enhanced from 53.4%, using only the venturi, to 59.9% using HC/H<sub>2</sub>O<sub>2</sub> with 0.5% as the optimal H<sub>2</sub>O<sub>2</sub> concentration. With 10 g L<sup>-1</sup> *p*-nitrophenol, no enhanced effect was observed due to the scavenging effects of unutilized hydrogen peroxide [125]. Thus, it can be said that H<sub>2</sub>O<sub>2</sub> is only favoured when it is used in optimum concentrations, which must be decided according to the concentration and type of pollutant as well as the cavitation intensity of the reactor, which all affect H<sub>2</sub>O<sub>2</sub> dissociation capacity [124].

#### 4.14. Enhanced effect of HC on Fenton oxidation

The HC/Fenton combination is most useful as a treatment of bio-refractory materials as it lowers toxicity to a certain level before conventional biological oxidation can be employed for final treatment. Higher pressures, the sequential addition of H<sub>2</sub>O<sub>2</sub> at higher loadings and lower effluent concentrations are favourable for rapid TOC mineralization [131].

For example, the treatment of diluted cooking wastewater using Fenton oxidation alone led to COD and polyphenol removal efficiencies of 30% and 61%, respectively. HC enhancement resulted in 83–90% increases in COD reduction and 26–33% increases in polyphenol reduction. The white biological films formed in cooking wastewater after HC/Fenton processing demonstrated that treated wastewater can be further purified using conventional biological process [133]. The degradation efficiency of organic pollutants using HC/Fenton are listed in Table 8.

The venturi system gave 99.9% degradation of 10 mg L<sup>-1</sup> Rhodamine B in a HC/Fenton combination (FeSO<sub>4</sub>:H<sub>2</sub>O<sub>2</sub> 1:5) at pH 2.5, as compared to 59.3% achieved with venturi alone, while 57% TOC was also removed [124]. As the FeSO<sub>4</sub>:H<sub>2</sub>O<sub>2</sub> ratio decreased from 1:0.5 to 1:4, the degradation of methyl parathion also increased in the presence of 100 mg L<sup>-1</sup> H<sub>2</sub>O<sub>2</sub> [126].

Similarly, 63.2% *p*-nitrophenol degradation was achieved by the HC/Fenton combination (FeSO<sub>4</sub>:H<sub>2</sub>O<sub>2</sub> 1:5) at pH 3.75, while HC alone provided 53.4%. Removal using the venturi system was higher than that using the orifice plate in combination with Fenton chemistry with 0.5 g L<sup>-1</sup> and 1 g L<sup>-1</sup> FeSO<sub>4</sub> at 1:5, 1:7.5 and 1:10 FeSO<sub>4</sub>:H<sub>2</sub>O<sub>2</sub> ratios. There was very little difference in removal value at pH 2.0 and pH 3.75, while the removal was 35.7% at pH 8. The generation of hydroxyl radicals by the decomposition of H<sub>2</sub>O<sub>2</sub> is favoured under acidic conditions and the oxidation capacity of hydroxyl radicals is also higher [124].

The physicochemical properties of pollutants, mainly their hydrophobicity and reactivity with hydroxyl radicals, obviously dominate the degradation efficacy of cavitation effects [124,134].

#### 4.15. Chemical process intensification by ultrasonic (acoustic) cavitation

##### 4.15.1. Organic reactions

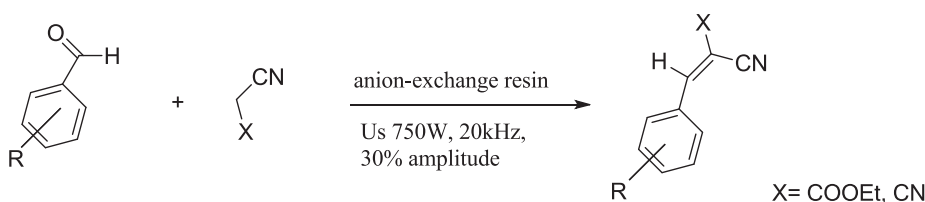
A few decades ago, the expertise gained from well-established extraction, processing and degradation techniques paved the way for the use of ultrasound as an alternative energy source in chemistry. The physical properties of the irradiated mixture are crucial for the effectiveness of cavitation and for the proper transfer of acoustic energy to reactants. The choice of a solvent that meets these requirements, while minimizing the environmental impact of the process, is therefore a fundamental one. Studies that combine sonochemistry with green, non-conventional solvents or that carry out the process with no solvents were surveyed by Lupacchini and co-authors in 2016 [135]. They

highlighted how the most frequently investigated options are water and ionic liquids, followed by ethylene glycol and its oligomers, glycerol and a few other biomass-derived solvents. Its intrinsic safety and environmental friendliness mean that water is the obvious benchmark for green solvents. Water and aqueous mixtures are the ideal environments for sonochemical reactions as cavitation is highly efficient at room temperature and at temperatures up to 50–60 °C. Furthermore, the use of large volumes of solvents of negligible cost favours process scalability. It is also worth noting that ultrasound helps to overcome reactant water solubility, which is particularly troublesome in organic synthesis and is a major limitation, by producing highly effective agitation and maximizing contact between phases.

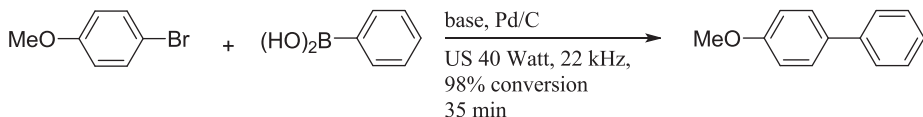
Catalysis in aqueous systems under sonochemical conditions has become an irreplaceable method for green synthetic chemistry after more than two decades of studies in this domain. The state-of-the-art was described by Cravotto *et al.* in 2015 [136], who gave a comprehensive overview of advantages and limitations as well as new potential applications. This review of sonochemical reactions in water (oxidation, bromination, aza-Michael, C–C couplings, MCR and aldol reactions) provided useful models with which to further the progress of organic synthesis using harmless and green sound energy. Catalytic procedures in water that are assisted by UC and/or HC are environmentally friendly and are performed under milder conditions, shorter reaction times and higher yields than many procedures. Sonochemical processes can reduce the formation of waste and hazardous by-products. Cavitation implosion generates mechanical and chemical effects, including the cleaning of catalyst surfaces and the formation of free radicals by water sonolysis.

The Knoevenagel condensation reaction is one of the most primitive routes for the synthesis of  $\alpha,\beta$ -unsaturated carbonyl compounds and occurs via the condensation of aldehydes or ketones with active methylene. Several Lewis bases and acids have also been reported to act as catalysts in the Knoevenagel condensation, but are hampered by difficult catalyst recovery and the generation of secondary products in most cases. Anion-exchange resins may be considered as insoluble bases, and might consequently be expected to advance reactions catalyzed by conventional bases. Solid catalysts work very well under UC and can be recycled several times, while sensitive molecules can, in some cases, react without polymerization or unwanted reactions. Ammar and co-authors developed a cleaner protocol for the Knoevenagel condensation of aromatic aldehydes with active methylene groups that is catalysed by anion-exchange resins under UC in 2015 [137]. All the reactions selectively produced the dehydrated products without any side reactions and self-condensation. Several aromatic aldehydes and various active methylene compounds, such as ethyl cyanoacetate and malononitrile, were reacted under UC at 20 kHz and room temperature, with a catalyst ratio = 0.25 g/0.01 mol, giving excellent yields (93–100%). When ethyl cyanoacetate was used as an active methylene compound, the reaction occurred with the stereoselective formation of E configured olefins with 100% selectivity. The reusability of the two resins was also investigated over four consecutive cycles of use. Compared with other reports, this method was more efficient and highlighted the significant role that ultrasound plays in the acceleration of chemical reactions at lower reaction temperatures (Scheme 1).

Palladium-catalyzed Suzuki-Miyaura coupling with aryl halides and arylboronic acids is a method of choice for the formation of biaryl units, which are a partial structure in many industrially important products. The literature presents many reports of sonochemical Suzuki-Miyaura cross-couplings that differ in terms of substrates, catalysts and the identification of reaction mechanisms. Sancheti *et al.* [138] have recently published an in depth investigation into the effects of the type of ultrasonic reactor used to promote the coupling and of operating parameters, such as ultrasonic power, temperature, catalyst loading and molar ratio, on these reactions and also provided some important information for industrial scale up. A simple model reaction of phenylboronic acid and 4-bromoanisole was successfully performed using



**Scheme 1.** Sonochemical Knoevenagel condensation.

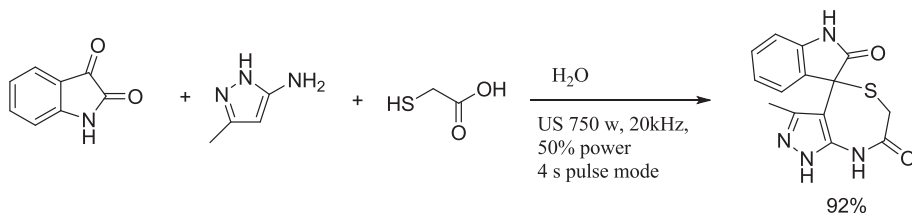


**Scheme 2.** Suzuki-Miyaura cross-coupling reaction of 4-bromoanisole.

Pd/C (5 wt% loading) in a 1:1 ethanol/water mixture. It was conclusively established that the reaction rate increased with increasing temperature over the 30 – 60 °C range and decreased beyond this temperature, when cavitation became progressively weaker, with lower intensity on bubble collapse. The overall optimum conditions established were: a molar ratio (phenylboronic acid: 4-bromoanisole) of 1.5 and a catalyst loading of 1.5 mol%, ultrasound power of 40 W and duty cycle of 90% at a frequency of 22 kHz, giving maximum conversion of 98% in only 35 min. The fact that the optimum power was 40 W is attributed to the lower energy that is actually transferred into the system at higher power dissipation levels due to the barrier created by large number of cavitation bubbles in the liquid leading to reduced cavitation intensity. The cavitation yield calculations revealed that the ultrasonic horn gave the maximum cavitation yield ( $28.21 \cdot 10^{-4}$  mg/J). This was followed by the ultrasonic bath without stirring ( $12.82 \cdot 10^{-4}$  mg/J), with the conventional approach giving the poorest results ( $9.6 \cdot 10^{-4}$  mg/J). Scale-up studies with reaction volumes that were 10 times larger also confirmed the excellent process intensification benefits that the UC assisted procedure provides (Scheme 2).

A convenient three-component reaction for the synthesis of spiro[indoline-3,4'-pyrazolo[3,4-e][1,4]thiazepines] was reported by Dandia *et al.* in 2013 [139]. The protocol used for the synthesis of this compound, which is important for medicinal chemistry, in high yields is a green multicomponent reaction of isatin, 5-amino-3-methylpyrazole and  $\alpha$ -mercaptocarboxylic acid in water that proceeds without a catalyst and is assisted by ultrasound irradiation (Scheme 3). The effect of ultrasound was examined and the results of reactions performed under silent conditions were compared with conventional stirring and heating. No reaction occurred under conventional stirring at room temperature and only a mixture of products was observed at a longer reaction time. By contrast, traces of product were monitored when the reaction was conducted at reflux. However, the result is not comparable with the 92% isolated product yield given by the ultrasound-assisted protocol in water. Thus, ultrasonic irradiation was found to have beneficial effects on the synthesis of a spiro[indoline-3,4'-pyrazolo[3,4-e][1,4]thiazepine]dione derivative that otherwise could not be synthesised by a catalyst-free protocol in water using conventional techniques.

In 2015, Ramazani *et al.* [140] developed an ultrasound promoted one-pot three-component reaction between *N*-isocyanaminotriphenylphosphorane, biacetyl and (*E*)-cinnamic acids for the synthesis of fully substituted 1,3,4-oxadiazole derivatives (Scheme



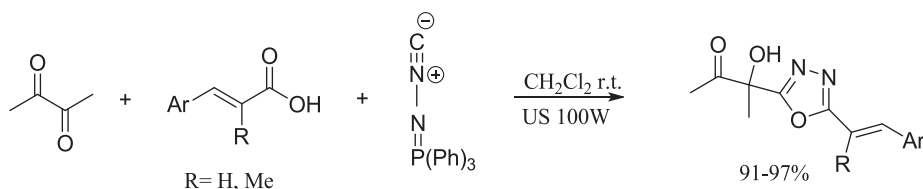
**Scheme 3.** Three component reaction for the synthesis of spiro[indoline-3,4'-pyrazolo[3,4-e][1,4]thiazepine].

4). The ultrasound-assisted methodology permitted the synthesis of the target molecule to occur with excellent yields (91–97%) within 16–27 min, whereas conventional stirring afforded the product in a comparable yield (85–92%), but with an extended reaction time (12 h). This significant step forwards in terms of reaction time and yields may be due to cavitation effects that improve mass transfer and create local temperature and pressure enhancements. Moreover, in this particular example, the nucleophilic addition of the *N*-isocyanaminotriphenyl phosphorane to biacetyl has a negative activation volume. Since negative activation volumes are accelerated under high pressure, the ultrasonic cavitation should have beneficial effects on this type of three-component reaction.

Another example reported in the literature is an ultrasound-promoted one-pot four component reaction used by Mahmoodi *et al.* in 2016 [141] for the synthesis of novel biologically active 3-aryl-2,4-dithioxo-1,3,5-triazepane-6,7-dione (Scheme 5). This protocol provides evidence for how ultrasound assisted reactions can dramatically reduce reaction times, proving that the technique can be used for more sustainable and greener methodologies as well as for process intensification.

An even more significant example of the importance of sonochemical reactions in organic synthesis was given by Saleh *et al.* in 2017 [142]. They reported a successful reaction for the synthesis of novel pyrano[3,4-e][1,3]oxazines under ultrasound irradiation that could not be carried out under silent conditions. 3-Benzyl-7-methyl-4-methylene-3,4-dihydropyrano[3,4-e][1,3]oxazine-2,5-dione was obtained in a 91% yield by reacting dimethyl carbonate and 3-(1-(benzylimino)ethyl)-4-hydroxy-6-methyl-2*H*-pyran-2-one for 45 min at 70–80 °C, using KF/basic alumina as the catalyst under sonochemical action (Scheme 6). No reaction occurred in the presence of the same catalyst and at the same reaction temperature under silent conditions, even after 12 h. It can therefore be stated that acoustic cavitation provided sufficient energy to the reactants to exceed the energy barrier of the reaction. The effect of cavitation at the solid-liquid interface can be interpreted by two mechanisms: the first is acoustic streaming, and the second microjet impact and shockwave damage. Acoustic streaming can simply be seen as the conversion of sound to kinetic energy, which aids mass transport. In the second case, the shockwaves and microjets associated with cavitation collapse cause localized deformation and surface erosion at the solid surface (catalyst), which increases the possible reaction area. Seeing as the reaction does not occur under silent conditions, the authors claim that this particular example might not only be driven by





**Scheme 4.** One-pot three-component reaction for the synthesis of fully substituted 1,3,4-oxadiazole derivatives.

kinetic energy, but that microjet impact and shockwave damage might also have a key role to play.

The synthesis of fatty acid methyl esters (FAME) via esterification or transesterification reactions has gained worldwide attention in recent years due to the development of a number of applications for the perfume and flavour industries and the use of biodiesel as a source of alternative fuel. In 2015, Dubey *et al.* presented a novel intensification approach for the synthesis of fatty acid methyl esters (FAME) from a non-edible high acid value Nagchampa oil (which contained higher amounts of the oil, 65–70%) using a two stage acid esterification reaction (catalysed by  $\text{H}_2\text{SO}_4$ , 1% w/w) followed by transesterification in the presence of a heterogeneous catalyst (CaO, 2.5% w/w)

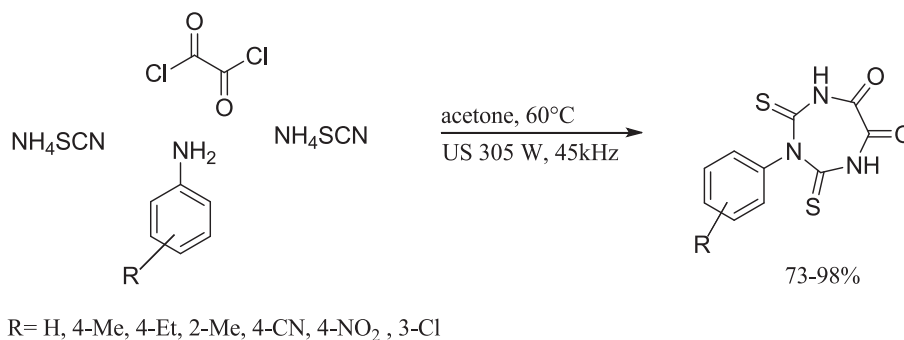
[143]. It was observed that FAME yield increases with an increase in CaO catalyst concentration from 1% to 2.5% (w/w). This yield increase can be attributed to increases in the number active sites in the reaction system. Further increases in catalyst concentration do not have a significant effect on the yield. The major problem associated with Nagchampa oil as a feedstock is its initial higher free fatty acid content, meaning that its processing is more like a two-stage approach; esterification (to reduce the free fatty acid content) followed by transesterification.

Another example of the ultrasonic fatty acid esterification of raw materials in heterogeneous catalysis has recently been described by Boffito *et al.* [144]. The authors report on the production of free fatty acid methyl esters from tobacco seed oil, refined canola oil and pure oleic acid in the presence of an acid ion exchange resin (Amberlyst® 46, A46) and analyse mass transfer in the heterogeneous reaction system using a kinetic model. The esterification method used can be considered a doubly-heterogeneous system with two phase boundaries; the catalyst-liquid boundary and the methanol surrounding the catalyst particle-oil boundary. In this respect, UC has been proven to be efficient in reducing mass transfer resistance at the solid-liquid interface via the formation of jets and shock waves induced by cavitation bubbles collapse. When compared with the conventional approach, the beneficial effects of ultrasound were more pronounced at lower temperatures. At 20 °C, the free fatty acid conversion of tobacco seed oil reached 68%, while conventional mechanical stirring achieved 23%. However, the conversion of the free fatty acids in tobacco seed oil approached about 70% at 63 °C, meaning that the ultrasound-assisted reaction gave results that were only slightly better than those of the conventionally heated reaction. The authors explained the data by stating that more gas is dissolved in liquid at low temperatures, thus generating more

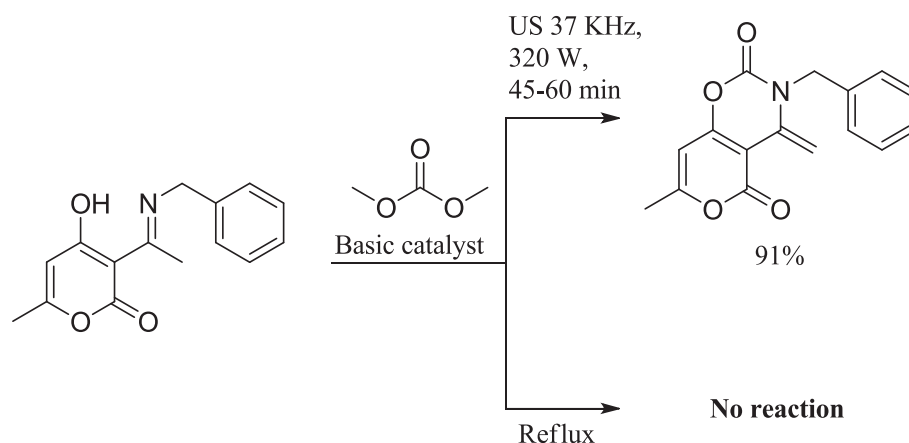
active nuclei for UC. Moreover, the viscosity of the medium is lower at low temperature and mass transfer resistance is also lower for conventional methods. Consequently, the two methods are comparable at 63 °C. The Eley–Rideal kinetic model, in which the concentration of the reacting species is expressed by taking into account the mass transfer between the phases, is in excellent agreement with the experimental data. Mass transfer coefficients were proven to be higher with ultrasound than under mechanical stirring, especially at 20 °C.

#### 4.16. Enzymatic catalysis

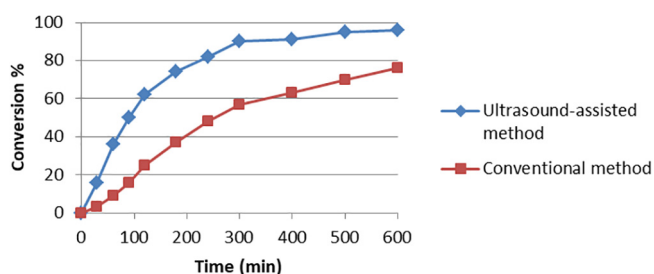
Microbial lipases occupy a prominent place among biocatalysts due to their ability to catalyze a wide variety of reactions in aqueous, non-aqueous media and solvent-free systems. The specific characteristics of these enzymes have generated interest among researchers as they catalyze reactions with reduced by-products, reduced waste treatment cost and mild temperature and pressure conditions. Ultrasound has also been used to extract and release intracellular enzymes and their subsequent activity can be further enhanced by the application of this technology. In 2017, Bansode *et al.* [145] debated the influence of ultrasound irradiation on reaction yield for different parameters, including temperature, enzyme concentration, molar substrate ratios, solvents, ultrasonic frequency and power. The workable ambient frequency for lipase catalysed reactions falls in the 20–40 kHz range in pulsating irradiation. An optimised temperature range, from 40 to 60 °C, is suitable for lipases as the enzymes undergo thermal denaturation at elevated temperatures, which affects their catalytic function. It is important that the active conformation of lipases remains intact and that no denaturation occurs due to increases in the concentrations of substrates or products around lipase. The higher substrate concentration with ultrasound provides faster rates and less accumulation of substrate at the proximity of lipases. This reduces the chances of the immediate denaturation of lipase and allows substrates to undergo improved interactions and increased collisions. A small amount of water is required for lipases to retain their catalytic conformation and flip into an active conformation. In the presence of ultrasound, the deleterious damage of solvents is minimised by the cavitation effects. A wide range of lipases can be used for many reactions of commercial importance. Of these, lipases from *Candida antarctica* are more stable and have been found to be tolerant to ultrasonic treatment. Chemical species (ions and free radicals) that are necessary to initiate or propagate the reaction are formed easily under ultrasound, and would



**Scheme 5.** 4-MCR synthesis of 3-(substituted phenyl)-2,4-dithioxo-1,3,5-triazepane-6,7-dione derivatives.



**Scheme 6.** Synthesis of pyrano[3,4-e][1,3]oxazine derivatives under ultrasonic irradiation.



**Fig. 5.** General trend of enzymatic reaction under conventional stirring and UC. The figure is inspired from Bansode and Rathod [136].

otherwise need extreme pressure and temperature conditions in conventional techniques. An evaluation of the impact of US with cavitation bubble dynamics can aid the further development of more optimised environments for scale up processes, reduced damage to biocatalysts and excellent yields. Applications of this technology for lipase-catalysed reactions are mainly: hydrolysis for free-fatty acid production, the esterification and transesterification of esters, alcoholysis for the production of biodiesel, glycerolysis for the production of mono and diglycerides, and polymerization Fig. 5.

## 5. Extractions

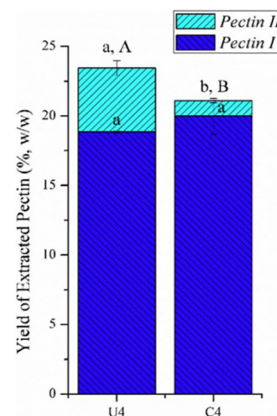
A key step for the sustainable exploitation of resources is the extraction method used.

- Ultrasound-assisted extraction (UAE) is a clean, environmentally friendly, fast, cost-effective and efficient alternative to traditional extraction techniques. UAE can benefit the extraction process as it provides the opportunity to use alternative (GRAS) (Generally Recognized As Safe) solvents by improving their extraction performance and enhancing the extraction of heat-sensitive components under conditions that would otherwise provide low yields. However, scale up to industrial applications still needs to be optimized. Tiwari [146] reported several examples of UAE using green solvents in 2015. The majority of reported extraction applications showed increases in extraction yield and reduced extraction times compared to conventional solid-liquid extraction (SLE) techniques. An example of acoustic-cavitation assisted extraction (ACAEE) was described in the literature by Wang *et al.* in 2017 [147]. The authors reported a green approach used for the two-stage extraction of pectin from waste grapefruit peels. Pectin is one of the ubiquitous biopolymers with high structural diversity that is found in the primary cell walls of terrestrial plants. Wang showed how the ACAEE

provides time and energy savings as it is a more effective method for the two-stage extraction of pectin from waste grapefruit peels than the conventional heating method. The results showed that a material particle size of 0.9 mm was sufficient to give an optimal pectin yield for ACAE. A potential general mechanism for the ACAEE of plant cell wall viscous polysaccharides was proposed and revealed the existence of a “barrier effect” during extraction. This was evidenced in the volume of residue per raw material weight (mL/g), which reflected the degree of disruption. When the pectin concentration in the extraction solution increased, a rise in mixture viscosity would induce an increase in cohesive forces, and thus a relative reduction in actual power intensity Fig. 6.

## 6. Conclusions

Cavitation chemistry has now become a mature discipline which interlinks physics, chemistry and chemical engineering. Reproducibility in green process intensification would still benefit greatly from a deeper understanding of the cavitation effects and an in-depth analysis of the phenomenon, in terms of physics and mathematics. Practitioners should bear in mind the importance of measurable UC and HC parameters and the influence of reactor design on experimental results. Their great potential in green chemistry and processing is still to be fully explored and exploited. It is hoped that the examples discussed in this review may stimulate scientists to work in this valuable research domain for years to come.



**Fig. 6.** Yield of extracted pectin after first and second stage extraction under different extraction conditions. U4: Ultrasound assisted extraction. C4: conventional extraction method. The figure is adapted and modified from Wang *et al.* [147].

## Acknowledgments

The present work was supported by the University of Turin (Ricerca locale 2017).

## References

- G. Cravotto, P. Cintas, Power ultrasound in organic synthesis: moving cavitation chemistry from academia to innovative and large-scale applications, *Chem. Soc. Rev.* 37 (2008) 2006–2027, <https://doi.org/10.1002/chin.200620271>.
- A.B. Pandit, J.B. Joshi, Hydrolysis of fatty oils: effect of cavitation, *Chem. Eng. Sci.* 48 (1993) 3440–3442.
- K.S. Suslick, M.M. Mdeleeni, J.T. Ries, Chemistry induced by hydrodynamic cavitation, *J. Am. Chem. Soc.* 119 (1997) 9303–9304, <https://doi.org/10.1021/ja972171i>.
- W.T. Richards, A.L. Loomis, The chemical effects of high frequency sound waves: i. a preliminary survey, *J. Am. Chem. Soc.* 49 (1927) 3086–3100, <https://doi.org/10.1021/ja01411a015>.
- F.O. Schmitt, C.H. Johnson, A.R. Olson, Oxidations promoted by ultrasonic radiation, *J. Am. Chem. Soc.* 51 (1929) 370–375, <https://doi.org/10.1021/ja01377a004>.
- S. Liu, H. Wu, Mechanism of oxidation promoted by ultrasonic radiation, *J. Am. Chem. Soc.* 56 (1934) 1005–1007.
- J.I. Thornycroft, S.W. Barnaby, Torpedo-boat destroyers, Minutes proceedings Institution civil engineers 122 (1895) 51–69, <https://doi.org/10.1680/imotp.1895.19693>.
- W.R. Moser, B.J. Marshik, J. Kingsley, M. Lemberger, R. Willette, A. Chan, J.E. Sunstrom, A. Boye, The synthesis and characterization of solid-state materials produced by high shear-hydrodynamic cavitation, *J. Mater. Res.* 10 (1995) 2322–2335, <https://doi.org/10.1557/jmr.1995.2322>.
- T.J. Mason, J.P. Lorimer, Applied sonochemistry: uses of power ultrasound in chemistry and processing, Wiley-VCH Verlag GmbH & Co. KGaA, Weinheim (2002), <https://doi.org/10.1002/352760054x>.
- J. Ji, J. Wang, Y. Li, Y. Yu, Z. Xu, Preparation of biodiesel with the help of ultrasonic and hydrodynamic cavitation, *Ultrasonics* 44 (2006) e411–e414, <https://doi.org/10.1016/j.ultras.2006.05.020>.
- A. Gedanken, Using sonochemistry for the fabrication of nanomaterials, *Ultrason. Sonochem.* 11 (2004) 47–55, <https://doi.org/10.1016/j.ulsonch.2004.01.037>.
- P.R. Gogate, Cavitation: an auxiliary technique in wastewater treatment schemes, *Adv. Environ. Res.* 6 (2002) 335–358.
- M. Zieliński, M. Dębowski, M. Kisielska, A. Nowicka, M. Rokicka, K. Szwarz, Comparison of ultrasonic and hydrothermal cavitation pretreatments of cattle manure mixed with straw wheat on fermentative biogas production, *Waste Biomass Valor.* (n.d.). doi:10.1007/s12649-017-9977-y.
- R.P.S. Suri, M. Nayak, U. Devaiah, E. Helmig, Ultrasound assisted destruction of estrogen hormones in aqueous solution: effect of power density, power intensity and reactor configuration, *J. Hazard. Mater.* 146 (2007) 472–478, <https://doi.org/10.1016/j.jhazmat.2007.04.072>.
- M. Sivakumar, A.B. Pandit, Ultrasound enhanced degradation of Rhodamine B: optimization with power density, *Ultrason. Sonochem.* 8 (2001) 233–240, [https://doi.org/10.1016/S1350-4177\(01\)00082-7](https://doi.org/10.1016/S1350-4177(01)00082-7).
- Z.-L. Wu, J. Lifka, B. Ondruschka, Comparison of energy efficiency of various ultrasonic devices in aquasonochemical reactions, *Chem. Eng. Technol.* 29 (2006) 610–615, <https://doi.org/10.1002/ceat.200500362>.
- S. Arrojo, Y. Benito, A.M. Tarifa, A parametrical study of disinfection with hydrodynamic cavitation, *Ultrason. Sonochem.* 15 (2008) 903–908, <https://doi.org/10.1016/j.ulsonch.2007.11.001>.
- W.-X. Li, C.-D. Tang, Z.-L. Wu, W.-M. Wang, Y.-F. Zhang, Y. Zhao, G. Cravotto, Eutrophic water purification efficiency using a combination of hydrodynamic cavitation and ozonation on a pilot scale, *Environ. Sci. Pollut. Res. Int.* 22 (2015) 6298.
- S. Arrojo, Y. Benito, A theoretical study of hydrodynamic cavitation, *Ultrason. Sonochem.* 15 (2008) 203–211, <https://doi.org/10.1016/j.ulsonch.2007.03.007>.
- P.R. Gogate, I.Z. Shirgaonkar, M. Sivakumar, P. Senthilkumar, N.P. Vichare, A.B. Pandit, Cavitation reactors: efficiency assessment using a model reaction, *AIChE J.* 47 (2001) 2526–2538, <https://doi.org/10.1002/aic.690471115>.
- P.R. Gogate, A.B. Pandit, A review and assessment of hydrodynamic cavitation as a technology for the future, *Ultrason. Sonochem.* 12 (2005) 21–27, <https://doi.org/10.1016/j.ulsonch.2004.03.007>.
- V.H. Arakeri, S. Chakraborty, Studies towards potential use of ultrasonics in hydrodynamic cavitation control, *Curr. Sci.* 1326–1333 (1990).
- A.L. Prajapat, P.R. Gogate, Intensified depolymerization of aqueous polyacrylamide solution using combined processes based on hydrodynamic cavitation, ozone, ultraviolet light and hydrogen peroxide, *Ultrason. Sonochem.* 31 (2016) 371–382.
- A. Shima, T. Tsujino, H. Nanjo, N. Miura, Cavitation damage in polymer aqueous solutions, *J. Fluids Eng.* 107 (1985) 134, <https://doi.org/10.1115/1.3242431>.
- K.K. Jyoti, A.B. Pandit, Water disinfection by acoustic and hydrodynamic cavitation, *Biochem. Eng. J.* 7 (2001) 201–212, [https://doi.org/10.1016/S1369-703X\(00\)00128-5](https://doi.org/10.1016/S1369-703X(00)00128-5).
- R.E.A. Arndt, Cavitation in fluid machinery and hydraulic structures, *Annu. Rev. Fluid Mech.* 13 (1981) 273–326, <https://doi.org/10.1146/annurev.fl.13.010181.001421>.
- Y.T. Shah, A.B. Pandit, V.S. Moholkar, Cavitation Reaction Engineering, Springer, Boston, MA (1999), <https://doi.org/10.1007/978-1-4615-4787-7>.
- F.G. R.T. Daily, J.W. Hammit Knapp, Cavitation. McGraw-Hill, New York, 1970.
- K. Morison, C. Hutchinson, Limitations of the Weissler reaction as a model reaction for measuring the efficiency of hydrodynamic cavitation, *Ultrason. Sonochem.* 16 (2009) 176–183, <https://doi.org/10.1016/j.ulsonch.2008.07.001>.
- V.L. Gole, K.R. Naveen, P.R. Gogate, Hydrodynamic cavitation as an efficient approach for intensification of synthesis of methyl esters from sustainable feedstock, *Chem. Eng. Process. Process Intensif.* 71 (2013) 70–76, <https://doi.org/10.1016/j.ccep.2012.10.006>.
- S.Y. Tang, M. Sivakumar, A novel and facile liquid whistle hydrodynamic cavitation reactor to produce submicron multiple emulsions, *AIChE J.* 59 (2013) 155–167, <https://doi.org/10.1002/aic.13800>.
- M.P. Badve, T. Alpar, A.B. Pandit, P.R. Gogate, L. Csoka, Modeling the shear rate and pressure drop in a hydrodynamic cavitation reactor with experimental validation based on KI decomposition studies, *Ultrason. Sonochem.* 22 (2015) 272–277, <https://doi.org/10.1016/j.ulsonch.2014.05.017>.
- Y.-F. Maa, C. Hsu, Liquid-liquid emulsification by rotor/stator homogenization, *J. Controlled Release.* 38 (1996) 219–228, [https://doi.org/10.1016/0168-3659\(95\)00123-9](https://doi.org/10.1016/0168-3659(95)00123-9).
- S. Rajorija, J. Carpenter, V.K. Saharan, A.B. Pandit, Hydrodynamic cavitation: an advanced oxidation process for the degradation of bio-refractory pollutants, *Rev. Chem. Eng.* 32 (2016) 379–411.
- Z. Zhang, G. Wang, Y. Nie, J. Ji, Hydrodynamic cavitation as an efficient method for the formation of sub-100 nm O/W emulsions with high stability, *Chin. J. Chem. Eng.* 24 (2016) 1477–1480, <https://doi.org/10.1016/j.cjche.2016.04.011>.
- J. Carpenter, S. George, V.K. Saharan, Low pressure hydrodynamic cavitation device for producing highly stable oil in water emulsion: Effect of geometry and cavitation number, *Chem. Eng. Process. Process Intensif.* 116 (2017) 97–104, <https://doi.org/10.1016/j.ccep.2017.02.013>.
- D. Ghayal, A.B. Pandit, V.K. Rathod, Optimization of biodiesel production in a hydrodynamic cavitation reactor using used frying oil, *Ultrason. Sonochem.* 20 (2013) 322–328, <https://doi.org/10.1016/j.ulsonch.2012.07.009>.
- M.J.A. Herrera, J. Malagónb, D.H. Prisciandard, M. Piemonte, V. Capocellic Ladino, Biodiesel production via hydrodynamic cavitation: numerical study of new geometrical arrangements, *Chem. Eng. Trans.* 50 (2016) 319–324, <https://doi.org/10.3303/CET1650054>.
- E.K. Spiridonov, S.Y. Bityutskikh, Characteristics and Analysis of a Cavitation Jet Mixer, *Chem. Pet. Eng.* 51 (2015) 226–232, <https://doi.org/10.1007/s10556-015-0028-x>.
- B. Freudig, S. Tesch, H. Schubert, Production of emulsions in high-pressure homogenizers – part ii: influence of cavitation on droplet breakup, *Eng. Life Sci.* 3 (2003) 266–270, <https://doi.org/10.1002/elsc.200390042>.
- S. Parthasarathy, T.S. Ying, S. Manickam, Generation and optimization of palm oil-based oil-in-water (o/w) submicron-emulsions and encapsulation of curcumin using a liquid whistle hydrodynamic cavitation reactor (LWHCR), *Ind. Eng. Chem. Res.* 52 (2013) 11829–11837, <https://doi.org/10.1021/ie4008858>.
- L.F. Chuah, S. Yusup, A.R.A. Aziz, A. Bokhari, M.Z. Abdullah, Cleaner production of methyl ester using waste cooking oil derived from palm olein using a hydrodynamic cavitation reactor, *J. Cleaner Prod.* 112 (2016) 4505–4514, <https://doi.org/10.1016/j.jclepro.2015.06.112>.
- W.R. Sunstrom, B. Moser, Marshik-Guerts, General route to nanocrystalline oxides by hydrodynamic cavitation, *Chem. Mater.* 8 (1996) 2061–2067, <https://doi.org/10.1021/cm950609c>.
- J. Find, S.C. Emerson, I.M. Krausz, W.R. Moser, Hydrodynamic cavitation as a tool to control macro-, micro-, and nano-properties of inorganic materials, *J. Mater. Res.* 16 (2001) 3503–3513, <https://doi.org/10.1557/jmr.2001.0481>.
- Z.A. Zhou, Z. Xu, J.A. Finch, H. Hu, S.R. Rao, Role of hydrodynamic cavitation in fine particle flotation, *Int. J. Miner. Process.* 51 (1997) 139–149, [https://doi.org/10.1016/S0301-7516\(97\)00026-4](https://doi.org/10.1016/S0301-7516(97)00026-4).
- Y.S. Ladola, S. Chowdhury, S.B. Roy, A.B. Pandit, Application of cavitation in uranium leaching, *Desalin. Water Treat.* 52 (2014) 407–414, <https://doi.org/10.1080/19443994.2013.808792>.
- P.R. Gogate, Cavitation reactors for process intensification of chemical processing applications: a critical review, *Chem. Eng. Process. Process Intensif.* 47 (2008) 515–527.
- V.G. Deshmane, P.R. Gogate, A.B. Pandit, Process intensification of synthesis process for medium chain glycerides using cavitation, *Chem. Eng. J.* 145 (2008) 351–354, <https://doi.org/10.1016/j.ccep.2008.08.012>.
- Z. Qiu, L. Zhao, L. Weatherley, Process intensification technologies in continuous biodiesel production, *Chem. Eng. Process. Process Intensif.* 49 (2010) 323–330, <https://doi.org/10.1016/j.ccep.2010.03.005>.
- A.L. Prajapat, P.R. Gogate, Intensification of depolymerization of aqueous guar gum using hydrodynamic cavitation, *Chem. Eng. Process. Process Intensif.* 93 (2015) 1–9, <https://doi.org/10.1016/j.ccep.2015.04.002>.
- L. Rinaldi, Z. Wu, S. Giovando, M. Bracco, D. Crudo, V. Bosco, G. Cravotto, Oxidative polymerization of waste cooking oil with air under hydrodynamic cavitation, *Green Process. Synth.* 6 (2017) 425–432, <https://doi.org/10.1515/gps-2016-0142>.
- K.B. Ansari, N.H. Loke, A.B. Pandit, V.G. Gaikar, R. Sivakumar, R. Kumar, S. Das, Process intensification of upgradation of crude oil and vacuum residue by hydrodynamic cavitation and microwave irradiation, *Indian Chem. Eng.* 57 (2015) 256–281. doi:10.1080/00194506.2015.1026949.
- N.B. Suryawanshi, V.M. Bhandari, L.G. Sorokhaibam, V.V. Ranade, Developing techno-economically sustainable methodologies for deep desulfurization using hydrodynamic cavitation, *Fuel.* 210 (2017) 482–490, <https://doi.org/10.1016/j.fuel.2017.08.106>.



- [54] P.R. Gogate, A.M. Kabadi, A review of applications of cavitation in biochemical engineering/biotechnology, *Biochem. Eng. J.* 44 (2009) 60–72.
- [55] G.D. Bosco, V. Cavaglià Giuliano, S. Mantegna, L.S. Battaglia, Cravotto Crudo, Process intensification in food industry: hydrodynamic and acoustic cavitation for fresh milk treatment *Agrofoodindustrytech* 25 (2014) 55–59.
- [56] K.E. Preece, N. Hooshyar, A.J. Krijgsman, P.J. Fryer, N.J. Zuidam, Intensification of protein extraction from soybean processing materials using hydrodynamic cavitation, *Innovative Food Sci. Emerg. Technol.* 41 (2017) 47–55, <https://doi.org/10.1016/j.ifset.2017.01.002>.
- [57] S. Roohinejad, M. Koubaa, F.J. Barba, R. Greiner, V. Orlien, N.I. Lebovka, Negative pressure cavitation extraction: a novel method for extraction of food bioactive compounds from plant materials, *Trends Food Sci. Technol.* 52 (2016) 98–108, <https://doi.org/10.1016/j.tifs.2016.04.005>.
- [58] P. Li, Y. Song, S. Yu, Removal of *Microcystis aeruginosa* using hydrodynamic cavitation: Performance and mechanisms, *Water Res.* 62 (2014) 241–248, <https://doi.org/10.1016/j.watres.2014.05.052>.
- [59] R.T. Hilares, D.V. Kamoei, M.A. Ahmed, S.S. da Silva, J.-I. Han, J.C. dos Santos, A new approach for bioethanol production from sugarcane bagasse using hydrodynamic cavitation assisted-pretreatment and column reactors, *Ultrason. Sonochem.* 43 (2018) 219–226, <https://doi.org/10.1016/j.ultsonch.2018.01.016>.
- [60] A. Iskalieva, B.M. Yimmou, P.R. Gogate, M. Horvath, P.G. Horvath, L. Csoka, Cavitation assisted delignification of wheat straw: a review, *Ultrason. Sonochem.* 19 (2012) 984–993, <https://doi.org/10.1016/j.ultsonch.2012.02.007>.
- [61] P.N. Patil, P.R. Gogate, L. Csoka, A. Dregelyi-Kiss, M. Horvath, Intensification of biogas production using pretreatment based on hydrodynamic cavitation, *Ultrason. Sonochem.* 30 (2016) 79–86, <https://doi.org/10.1016/j.ultsonch.2015.11.009>.
- [62] M.P. Badve, M.N. Bhagat, A.B. Pandit, Microbial disinfection of seawater using hydrodynamic cavitation, *Sep. Purif. Technol.* 151 (2015) 31–38.
- [63] W. Zhu, C. Wu, L. Chen, G. Wu, Influence factors of phenol degradation in water by ozonation with enhancement of hydrodynamic cavitation, *Ind. Water Wastewater* 38 (2007) 23.
- [64] P.R. Gogate, G.S. Bhosale, Comparison of effectiveness of acoustic and hydrodynamic cavitation in combined treatment schemes for degradation of dye wastewaters, *Chem. Eng. Process. Process Intensif.* 71 (2013) 59–69, <https://doi.org/10.1016/j.ccep.2013.03.001>.
- [65] P. Thanekar, M. Panda, P.R. Gogate, Degradation of carbamazepine using hydrodynamic cavitation combined with advanced oxidation processes, *Ultrason. Sonochem.* 40 (2018) 567–576, <https://doi.org/10.1016/j.ultsonch.2017.08.001>.
- [66] M.Á. Cerqueira, A.C. Pinheiro, O.L. Ramos, H. Silva, A.I. Bourbon, A.A. Vicente, Chapter Two - Advances in Food Nanotechnology, *Emerging Nanotechnologies Food Science, Micro Nano Technologies* (2017) 11–38, <https://doi.org/10.1016/b978-0-323-42980-1.00002-9>.
- [67] B. Abismail, J.P. Canselier, A.M. Wilhelm, H. Delmas, C. Gourdon, Emulsification by ultrasound: drop size distribution and stability, *Ultrason. Sonochem.* 6 (1999) 75–83, [https://doi.org/10.1016/s1350-4177\(98\)00027-3](https://doi.org/10.1016/s1350-4177(98)00027-3).
- [68] V.A. Burmistrov, I.M. Lipatova, N.V. Losev, J.A. Rodicheva, O.I. Koifman, Influence of the composition and high shear stresses on the structure and properties of hybrid materials based on starch and synthetic copolymer, *Carbohydr. Polym.* 196 (2018) 368–375, <https://doi.org/10.1016/j.carbpol.2018.05.056>.
- [69] I. Burgaud, E. Dickinson, P.V. Nelson, An improved high-pressure homogenizer for making fine emulsions on a small scale, *Int. J. Food Sci. Technol.* 25 (1990) 39–46, <https://doi.org/10.1111/j.1365-2621.1990.tb01057.x>.
- [70] O.V. Kozyuk, Use of hydrodynamic cavitation for emulsifying and homogenizing processes, *Am. Lab.* 31 (1999) 6–7.
- [71] K.A. Ramisetty, A.B. Pandit, P.R. Gogate, Novel approach of producing oil in water emulsion using hydrodynamic cavitation reactor, *Ind. Eng. Chem. Res.* 53 (2014) 16508–16515, <https://doi.org/10.1021/ie502753d>.
- [72] G. Cravotto, I. Choedkiatsakul, Combined Enabling Technologies for Biodiesel Production in Flow Processes, in: J.X.Q. Zhen, Fang Richard, L. Smith (Ed.), Springer, Springer, Dordrecht, 2015: pp. 41–57. doi:10.1007/978-94-017-9612-5\_3.
- [73] L.F. Chuah, J.J. Klemeš, S. Yusup, A. Bokhari, M.M. Akbar, A review of cleaner intensification technologies in biodiesel production, *J. Cleaner Prod.* 146 (2017) 181–193, <https://doi.org/10.1016/j.jclepro.2016.05.017>.
- [74] L.F. Chuah, J.J. Klemeš, S. Yusup, A. Bokhari, M.M. Akbar, Z.K. Chong, Kinetic studies on waste cooking oil into biodiesel via hydrodynamic cavitation, *J. Cleaner Prod.* 146 (2017) 47–56, <https://doi.org/10.1016/j.jclepro.2016.06.187>.
- [75] B. Sajjadi, A.R.A. Aziz, S. Ibrahim, Mechanistic analysis of cavitation assisted transesterification on biodiesel characteristics, *Ultrason. Sonochem.* 22 (2015) 463–473, <https://doi.org/10.1016/j.ultsonch.2014.06.004>.
- [76] A. Bokhari, L.F. Chuah, S. Yusup, J.J. Klemeš, R.N.M. Kamil, Optimisation on pretreatment of rubber seed (*Hevea brasiliensis*) oil via esterification reaction in a hydrodynamic cavitation reactor, *Bioresour. Technol.* 199 (2016) 414–422, <https://doi.org/10.1016/j.biortech.2015.08.013>.
- [77] A. Pal, A. Verma, S.S. Kachhwaha, S. Maji, Biodiesel production through hydrodynamic cavitation and performance testing, *Renew. Energ.* 35 (2010) 619–624, <https://doi.org/10.1016/j.renene.2009.08.027>.
- [78] G.L. Maddikeri, P.R. Gogate, A.B. Pandit, Intensified synthesis of biodiesel using hydrodynamic cavitation reactors based on the inter esterification of waste cooking oil 137 (2014) 285–292, <https://doi.org/10.1016/j.fuel.2014.08.013>.
- [79] J.S. Bokhari, A. Chuah, L.F. Ahmad Yusup, Pre-blended methyl esters production from crude palm and rubber seed oil via hydrodynamic cavitation reactor, *Chem. Eng. Trans.* 43 (2015).
- [80] V.S. Moholkar, P.S. Kumar, A.B. Pandit, Hydrodynamic cavitation for sonochemical effects, *Ultrason. Sonochem.* 6 (1999) 53–65, [https://doi.org/10.1016/s1350-4177\(98\)00030-3](https://doi.org/10.1016/s1350-4177(98)00030-3).
- [81] P.M. Kanthale, P.R. Gogate, A.B. Pandit, A.M. Wilhelm, Mapping of an ultrasonic horn: link primary and secondary effects of ultrasound, *Ultrason. Sonochem.* 10 (2003) 331–335, [https://doi.org/10.1016/s1350-4177\(03\)00104-4](https://doi.org/10.1016/s1350-4177(03)00104-4).
- [82] V.L. Gole, P.R. Gogate, A review on intensification of synthesis of biodiesel from sustainable feed stock using sonochemical reactors, *Chem. Eng. Process. Process Intensif.* 53 (2012) 1–9, <https://doi.org/10.1016/j.ccep.2011.12.008>.
- [83] M.A. Kelkar, P.R. Gogate, A.B. Pandit, Intensification of esterification of acids for synthesis of biodiesel using acoustic and hydrodynamic cavitation, *Ultrason. Sonochem.* 15 (2008) 188–194, <https://doi.org/10.1016/j.ultsonch.2007.04.003>.
- [84] A.V. Mohod, A.S. Subudhi, P.R. Gogate, Intensification of esterification of non edible oil as sustainable feedstock using cavitation reactors, *Ultrason. Sonochem.* 36 (2017) 309–318, <https://doi.org/10.1016/j.ultsonch.2016.11.040>.
- [85] P.M. Ondruschka, B. Braeutigam Franke, Hydrodynamic-acoustic-cavitation for biodiesel synthesis, in: 3rd International Conference Environment, Chemistry/Biology, 2014: pp. 23–30.
- [86] G.L. Maddikeri, A.B. Pandit, P.R. Gogate, Ultrasound assisted interesterification of waste cooking oil and methyl acetate for biodiesel and triacetin production, *Fuel Process. Technol.* 116 (2013) 241–249, <https://doi.org/10.1016/j.fuproc.2013.07.004>.
- [87] L.F. Chuah, S. Yusup, A.R.A. Aziz, A. Bokhari, J.J. Klemeš, M.Z. Abdullah, Intensification of biodiesel synthesis from waste cooking oil (Palm Olein) in a Hydrodynamic Cavitation Reactor: Effect of operating parameters on methyl ester conversion, *Chem. Eng. Process. Process Intensif.* 95 (2015) 235–240, <https://doi.org/10.1016/j.ccep.2015.06.018>.
- [88] K.M. Kumar, E.T.P. Sathesh, T. Venkadesh, D. Kumaraguru Rengasamy, Hydrodynamic cavitation for the production of biodiesel from sunflower oil using NaOH catalyst, *J. Chem. Pharmaceutical Sci.* (2014) 104–106.
- [89] A. Bokhari, S. Yusup, L.F. Chuah, J.J. Klemeš, S. Asif, B. Ali, M.M. Akbar, R.N.M. Kamil, Pilot scale intensification of rubber seed (*Hevea brasiliensis*) oil via chemical interesterification using hydrodynamic cavitation technology, *Bioresour. Technol.* 242 (2017) 272–282, <https://doi.org/10.1016/j.biortech.2017.03.046>.
- [90] D. Crudo, V. Bosco, G. Cavaglià, G. Grillo, S. Mantegna, G. Cravotto, Biodiesel production process intensification using a rotor-stator type generator of hydrodynamic cavitation, *Ultrason. Sonochem.* 33 (2016) 220–225, <https://doi.org/10.1016/j.ultsonch.2016.05.001>.
- [91] A.V. Mohod, P.R. Gogate, G. Viel, P. Firmino, R. Giudici, Intensification of biodiesel production using hydrodynamic cavitation based on high speed homogenizer, *Chem. Eng. J.* 316 (2017) 751–757, <https://doi.org/10.1016/j.cej.2017.02.011>.
- [92] S. Joshi, P.R. Gogate, P.F. Moreira, R. Giudici, Intensification of biodiesel production from soybean oil and waste cooking oil in the presence of heterogeneous catalyst using high speed homogenizer, *Ultrason. Sonochem.* 39 (2017) 645–653, <https://doi.org/10.1016/j.ultsonch.2017.05.029>.
- [93] V. Bosco, D. Crudo, Dispositivo e metodo per il trattamento di fluidi mediante cavitazione idrodinamica (Device and method for the treatment of fluids by hydrodynamic cavitation), Italian patent 10201600007489, 2018.
- [94] A. Bokhari, L.F. Chuah, S. Yusup, J.J. Klemeš, M.M. Akbar, R.N.M. Kamil, Cleaner production of rubber seed oil methyl ester using a hydrodynamic cavitation: optimisation and parametric study, *J. Cleaner Prod.* 136 (2016) 31–41, <https://doi.org/10.1016/j.jclepro.2016.04.091>.
- [95] P.R. Gogate, A.B. Pandit, A review of imperative technologies for wastewater treatment I: oxidation technologies at ambient conditions, *Adv. Environ. Res.* 8 (2004) 501–551.
- [96] M.M. Huber, S. Canonica, G.-Y. Park, U. Von Gunten, Oxidation of pharmaceuticals during ozonation and advanced oxidation processes, *Environ. Sci. Technol.* 37 (2003) 1016–1024.
- [97] Y.W. Kang, K.-Y. Hwang, Effects of reaction conditions on the oxidation efficiency in the Fenton process, *Water Res.* 34 (2000) 2786–2790, [https://doi.org/10.1016/s0043-1354\(99\)00388-7](https://doi.org/10.1016/s0043-1354(99)00388-7).
- [98] M.R. Hoffmann, S.T. Martin, W. Choi, D.W. Bahnemann, Environmental applications of semiconductor photocatalysis, *Chem. Rev.* 95 (1995) 69–96, <https://doi.org/10.1021/cr00033a004>.
- [99] P.R. Gogate, A.B. Pandit, Hydrodynamic cavitation reactors: a state of the art review, *Rev. Chem. Eng.* 17 (2001) 1–85, <https://doi.org/10.1515/REVCE.2001.17.1.1>.
- [100] L.P. Amin, P.R. Gogate, A.E. Burgess, D.H. Bremner, Optimization of a hydrodynamic cavitation reactor using salicylic acid dosimetry, *Chem. Eng. J.* 156 (2010) 165–169, <https://doi.org/10.1016/j.cej.2009.09.043>.
- [101] Z.-L. Wu, B. Ondruschka, P. Bräutigam, Degradation of chlorocarbons driven by hydrodynamic cavitation, *Chem. Eng. Technol.* 30 (2007) 642–648, <https://doi.org/10.1002/ceat.200600288>.
- [102] Z. Wu, B. Ondruschka, Y. Zhang, D.H. Bremner, H. Shen, M. Franke, Chemistry driven by suction, *Green Chem.* 11 (2009) 1026, <https://doi.org/10.1039/b902224d>.
- [103] M. Franke, P. Braeutigam, Z.-L. Wu, Y. Ren, B. Ondruschka, Enhancement of chloroform degradation by the combination of hydrodynamic and acoustic cavitation, *Ultrason. Sonochem.* 18 (2011) 888–894, <https://doi.org/10.1016/j.ultsonch.2010.11.011>.
- [104] K.M. Kalumuck, G.L. Chahine, The use of cavitating jets to oxidize organic compounds in water, *J. Fluids Eng.* 122 (2000) 465–470, <https://doi.org/10.1115/1.1286993>.
- [105] M. Sivakumar, A.B. Pandit, Wastewater treatment: a novel energy efficient hydrodynamic cavitation technique, *Ultrason. Sonochem.* 9 (2002) 123–131, [https://doi.org/10.1016/s1350-4177\(01\)00122-5](https://doi.org/10.1016/s1350-4177(01)00122-5).
- [106] D.H. Bremner, S.D. Carlo, A.G. Chakinala, G. Cravotto, Mineralisation of 2,4-



- dichlorophenoxyacetic acid by acoustic or hydrodynamic cavitation in conjunction with the advanced Fenton process, *Ultrason. Sonochem.* 15 (2008) 416–419, <https://doi.org/10.1016/j.ulsonch.2007.06.003>.
- [107] J. Choi, M. Cui, Y. Lee, J. Kim, Y. Son, J. Khim, Hydrodynamic cavitation and activated persulfate oxidation for degradation of bisphenol A: kinetics and mechanism, *Chem. Eng. J.* 338 (2018) 323–332, <https://doi.org/10.1016/j.cej.2018.01.018>.
- [108] M.V. Bagal, P.R. Gogate, Degradation of 2,4-dinitrophenol using a combination of hydrodynamic cavitation, chemical and advanced oxidation processes, *Ultrason. Sonochem.* 20 (2013) 1226–1235, <https://doi.org/10.1016/j.ulsonch.2013.02.004>.
- [109] P.N. Patil, S.D. Bote, P.R. Gogate, Degradation of imidacloprid using combined advanced oxidation processes based on hydrodynamic cavitation, *Ultrason. Sonochem.* 21 (2014) 1770–1777.
- [110] S. Khoei, H. Fakhri, C.B. Canbolat, T. Olmez-Hanci, B. Keskinler, Treatment of medium density fiberboard wastewater by Fe<sup>2+</sup>/persulfate and Fe<sup>2+</sup>/persulfate enhanced hydrodynamic cavitation processes, *Fresenius Environ. Bull.* 26 (2017) 483–489.
- [111] N.H. Ince, G. Tezcanli, R.K. Belen, İ.G. Apikyan, Ultrasound as a catalyzer of aqueous reaction systems: the state of the art and environmental applications, *Appl. Catal., B* 29 (2001) 167–176. doi:10.1016/S0926-3373(00)00224-1.
- [112] L.H. Thompson, L.K. Doraiswamy, Sonochemistry: science and engineering, *Ind. Eng. Chem. Res.* 38 (1999) 1215–1249, <https://doi.org/10.1021/ie9804172>.
- [113] E.F. Karamah, S. Bismo, W.W. Purwanto, Significance of acoustic and hydrodynamic cavitations in enhancing ozone mass transfer, *Ozone Sci. Eng.* 35 (2013) 482–488.
- [114] L.-B. Chu, X.-H. Xing, A.-F. Yu, Y.-N. Zhou, X.-L. Sun, B. Jurcik, Enhanced ozonation of simulated dyestuff wastewater by microbubbles, *Chemosphere* 68 (2007) 1854–1860, <https://doi.org/10.1016/j.chemosphere.2007.03.014>.
- [115] Z. Wu, H. Shen, B. Ondruschka, Y. Zhang, W. Wang, D.H. Bremner, Removal of blue-green algae using the hybrid method of hydrodynamic cavitation and ozonation, *J. Hazard. Mater.* 235 (2012) 152–158.
- [116] Z. Wu, M. Franke, B. Ondruschka, Y. Zhang, Y. Ren, P. Braeutigam, W. Wang, Enhanced effect of suction-cavitation on the ozonation of phenol, *J. Hazard. Mater.* 190 (2011) 375–380.
- [117] Z. Wu, G. Cravotto, B. Ondruschka, A. Stolle, W. Li, Decomposition of chloroform and succinic acid by ozonation in a suction-cavitation system: Effects of gas flow, *Sep. Purif. Technol.* 161 (2016) 25–31.
- [118] S.S. Sawant, A.C. Anil, V. Krishnamurthy, C. Gaonkar, J. Kolwalkar, L. Khandeparker, D. Desai, A.V. Mahulkar, V.V. Ranade, A.B. Pandit, Effect of hydrodynamic cavitation on zooplankton: a tool for disinfection, *Chem. Eng. J.* 42 (2008) 320–328, <https://doi.org/10.1016/j.bej.2008.08.001>.
- [119] L. Mezule, S. Tsyfansky, V. Yakushevich, T. Juhna, A simple technique for water disinfection with hydrodynamic cavitation: effect on survival of *Escherichia coli*, *Desalination* 248 (2009) 152–159, <https://doi.org/10.1016/j.desal.2008.05.051>.
- [120] I. Lee, J.-I. Han, Simultaneous treatment (cell disruption and lipid extraction) of wet microalgae using hydrodynamic cavitation for enhancing the lipid yield, *Bioresour. Technol.* 186 (2015) 246–251, <https://doi.org/10.1016/j.biortech.2015.03.045>.
- [121] P. Braeutigam, Z.-L. Wu, A. Stark, B. Ondruschka, Degradation of btx in aqueous solution by hydrodynamic cavitation, *Chem. Eng. Technol.* 32 (2009) 745–753, <https://doi.org/10.1002/ceat.200800626>.
- [122] X. Wang, Y. Zhang, Degradation of alachlor in aqueous solution by using hydrodynamic cavitation, *J. Hazard. Mater.* 161 (2009) 202–207, <https://doi.org/10.1016/j.jhazmat.2008.03.073>.
- [123] V.K. Saharan, A.B. Pandit, P.S. Satish Kumar, S. Anandan, Hydrodynamic cavitation as an advanced oxidation technique for the degradation of Acid Red 88 dye, *Ind. Eng. Chem. Res.* 51 (2011) 1981–1989.
- [124] K.P. Mishra, P.R. Gogate, Intensification of degradation of Rhodamine B using hydrodynamic cavitation in the presence of additives, *Sep. Purif. Technol.* 75 (2010) 385–391, <https://doi.org/10.1016/j.seppur.2010.09.008>.
- [125] A.A. Pradhan, P.R. Gogate, Removal of p-nitrophenol using hydrodynamic cavitation and Fenton chemistry at pilot scale operation, *Chem. Eng. J.* 156 (2010) 77–82, <https://doi.org/10.1016/j.cej.2009.09.042>.
- [126] P.N. Patil, P.R. Gogate, Degradation of methyl parathion using hydrodynamic cavitation: effect of operating parameters and intensification using additives, *Sep. Purif. Technol.* 95 (2012) 172–179.
- [127] M. Zupanc, T. Kosjek, M. Petkovšek, M. Dular, B. Kompare, B. Širok, Ž. Blažeka, E. Heath, Removal of pharmaceuticals from wastewater by biological processes, hydrodynamic cavitation and UV treatment, *Ultrason. Sonochem.* 20 (2013) 1104–1112.
- [128] A.G. Chakinala, D.H. Bremner, P.R. Gogate, K.-C. Namkung, A.E. Burgess, Multivariate analysis of phenol mineralisation by combined hydrodynamic cavitation and heterogeneous advanced Fenton processing, *Appl. Catal., B* 78 (2008) 11–18, <https://doi.org/10.1016/j.apcatb.2007.08.012>.
- [129] P.R. Gogate, A.B. Pandit, Engineering design method for cavitation reactors: I. Sonochemical reactors, *AIChE J.* 46 (2000) 372–379, <https://doi.org/10.1002/aic.690460215>.
- [130] M. Goel, H. Hongqiang, A.S. Mujumdar, M.B. Ray, Sonochemical decomposition of volatile and non-volatile organic compounds—a comparative study, *Water Res.* 38 (2004) 4247–4261, <https://doi.org/10.1016/j.watres.2004.08.008>.
- [131] A.G. Chakinala, P.R. Gogate, A.E. Burgess, D.H. Bremner, Treatment of industrial wastewater effluents using hydrodynamic cavitation and the advanced Fenton process, *Ultrason. Sonochem.* 15 (2008) 49–54.
- [132] X. Wang, J. Wang, P. Guo, W. Guo, C. Wang, Degradation of rhodamine B in aqueous solution by using swirling jet-induced cavitation combined with H<sub>2</sub>O<sub>2</sub>, *J. Hazard. Mater.* 169 (2009) 486–491.
- [133] Z. Wu, F.J. Yuste-Córdoba, P. Cintas, Z. Wu, L. Boffa, S. Mantegna, G. Cravotto, Effects of ultrasonic and hydrodynamic cavitation on the treatment of cork wastewater by flocculation and Fenton processes, *Ultrason. Sonochem.* 40 (2018) 3–8, <https://doi.org/10.1016/j.ulsonch.2017.04.016>.
- [134] Z. Wu, B. Ondruschka, Roles of Hydrophobicity and Volatility of Organic Substrates on Sonolytic Kinetics in Aqueous Solutions, *J. Phys. Chem. A* 109 (2005) 6521–6526, <https://doi.org/10.1021/jp051768e>.
- [135] M. Lupacchini, A. Mascitti, G. Giachi, L. Tonucci, N.d. Alessandro, J. Martinez, E. Colacino, Sonochemistry in non-conventional, green solvents or solvent-free reactions, *Tetrahedron* 73 (2017) 609–653, <https://doi.org/10.1016/j.tet.2016.12.014>.
- [136] G. Cravotto, E. Borretto, M. Oliverio, A. Procopio, A. Penoni, Organic reactions in water or biphasic aqueous systems under sonochemical conditions. A review on catalytic effects, *Catal. Commun.* 63 (2015) 2–9, <https://doi.org/10.1016/j.catcom.2014.12.014>.
- [137] H.B. Ammar, M. Chtourou, M.H. Frikha, M. Trabelsi, Green condensation reaction of aromatic aldehydes with active methylene compounds catalyzed by anion-exchange resin under ultrasound irradiation, *Ultrason. Sonochem.* 22 (2015) 559–564, <https://doi.org/10.1016/j.ulsonch.2014.07.018>.
- [138] S.V. Sancheti, P.R. Gogate, Intensification of heterogeneously catalyzed Suzuki-Miyaura cross-coupling reaction using ultrasound: understanding effect of operating parameters, *Ultrason. Sonochem.* 40 (2018) 30–39, <https://doi.org/10.1016/j.ulsonch.2017.01.037>.
- [139] A. Dandia, R. Singh, J. Joshi, S. Maheshwari, P. Soni, Ultrasound promoted catalyst-free and selective synthesis of spiro[indole-3,4'-pyrazolo[3,4-e][1,4]thiazepines] in aqueous media and evaluation of their anti-hyperglycemic activity, *RSCAdv.* 3 (2013) 18992, <https://doi.org/10.1039/c3ra43745k>.
- [140] A. Ramazani, M. Rouhani, F.Z. Nasrabi, F. Gouranlou, Ultrasound-Promoted Three-Component Reaction of N-isocyaniminotriphenyl-phosphorane, (E)-cinamic Acids, and Biacetyl, *Sulfur Silicon Relat. Elem.* 190 (2015) 20–28, <https://doi.org/10.1080/10426507.2014.909428>.
- [141] N.O. Mahmoodi, M.M. Zeydi, E. Biazar, Ultrasound-promoted one-pot four-component synthesis of novel biologically active 3-aryl-2,4-dithioxo-1,3,5-triazepane-6,7-dione and their toxicity investigation, *J. Sulfur Chem.* 37 (2016) 613–621, <https://doi.org/10.1080/17415993.2016.1169534>.
- [142] T.S. Saleh, A.S. Al-Bogami, A.E.M. Mekky, H.Z. Alkhatlan, Sonochemical synthesis of novel pyrano[3,4-e][1,3]oxazines: a green protocol, *Ultrason. Sonochem.* 36 (2017) 474–480, <https://doi.org/10.1016/j.ulsonch.2016.12.015>.
- [143] S.M. Dubey, V.L. Gole, P.R. Gogate, Cavitation assisted synthesis of fatty acid methyl esters from sustainable feedstock in presence of heterogeneous catalyst using two step process, *Ultrason. Sonochem.* 23 (2015) 165–173, <https://doi.org/10.1016/j.ulsonch.2014.08.019>.
- [144] D.C. Boffito, F. Galli, C. Pirola, C.L. Bianchi, G.S. Patience, Ultrasonic free fatty acids esterification in tobacco and canola oil, *Ultrason. Sonochem.* 21 (2014) 1969–1975, <https://doi.org/10.1016/j.ulsonch.2014.01.026>.
- [145] S.R. Bansode, V.K. Rathod, An investigation of lipase catalysed sonochemical synthesis: A review, *Ultrason. Sonochem.* 38 (2017) 503–529, <https://doi.org/10.1016/j.ulsonch.2017.02.028>.
- [146] B.K. Tiwari, Ultrasound: a clean, green extraction technology, *Trends Anal. Chem.* 71 (2015) 100–109, <https://doi.org/10.1016/j.trac.2015.04.013>.
- [147] W. Wang, X. Ma, Y. Xu, Y. Cao, Z. Jiang, T. Ding, X. Ye, D. Liu, Ultrasound-assisted heating extraction of pectin from grapefruit peel: Optimization and comparison with the conventional method, *FoodChem.* 178 (2015) 106–114, <https://doi.org/10.1016/j.foodchem.2015.01.080>.